

Review



**Cite this article:** Jørgensen *ACS et al.* 2023

Data-driven spatio-temporal modelling of glioblastoma. *R. Soc. Open Sci.* **10**: 221444.

<https://doi.org/10.1098/rsos.221444>

Received: 8 November 2022

Accepted: 23 February 2023

**Subject Category:**

Mathematics

**Subject Areas:**

computational biology/mathematical modelling

**Keywords:**

agent-based modelling, glioblastoma, reaction–diffusion equations, Bayesian inference, data-driven modelling

**Authors for correspondence:**

Andreas Christ Sølvesten Jørgensen

e-mail: [a.jorgensen@imperial.ac.uk](mailto:a.jorgensen@imperial.ac.uk)

Vahid Shahrezaei

e-mail: [v.shahrezaei@imperial.ac.uk](mailto:v.shahrezaei@imperial.ac.uk)

# Data-driven spatio-temporal modelling of glioblastoma

Andreas Christ Sølvesten Jørgensen<sup>1</sup>, Ciaran Scott Hill<sup>2,3</sup>, Marc Sturrock<sup>4</sup>, Wenhao Tang<sup>1</sup>, Saketh R. Karamched<sup>5</sup>, Dunja Gorup<sup>5</sup>, Mark F. Lythgoe<sup>5</sup>, Simona Parrinello<sup>3</sup>, Samuel Marguerat<sup>6</sup> and Vahid Shahrezaei<sup>1</sup>

<sup>1</sup>Department of Mathematics, Faculty of Natural Sciences, Imperial College London, London SW7 2AZ, UK


<sup>2</sup>Department of Neurosurgery, The National Hospital for Neurology and Neurosurgery, London WC1N 3BG, UK

<sup>3</sup>Samantha Dickson Brain Cancer Unit, UCL Cancer Institute, London WC1E 6DD, UK

<sup>4</sup>Department of Physiology and Medical Physics, Royal College of Surgeons in Ireland, Dublin D02 YN77, Ireland

<sup>5</sup>Division of Medicine, Centre for Advanced Biomedical Imaging, University College London (UCL), London WC1E 6BT, UK

<sup>6</sup>Genomics Translational Technology Platform, UCL Cancer Institute, University College London, London WC1E 6DD, UK

 ACSJ, 0000-0003-2276-5779; CSH, 0000-0002-4488-4034; MS, 0000-0002-7435-5256; WT, 0000-0002-4063-0846; SRK, 0000-0003-4031-5915; DG, 0000-0002-3756-7452; MFL, 0000-0002-4945-0171; SP, 0000-0003-0820-6292; SM, 0000-0002-2402-3165; VS, 0000-0002-4013-5458

Mathematical oncology provides unique and invaluable insights into tumour growth on both the microscopic and macroscopic levels. This review presents state-of-the-art modelling techniques and focuses on their role in understanding glioblastoma, a malignant form of brain cancer. For each approach, we summarize the scope, drawbacks and assets. We highlight the potential clinical applications of each modelling technique and discuss the connections between the mathematical models and the molecular and imaging data used to inform them. By doing so, we aim to prime cancer researchers with current and emerging computational tools for understanding tumour progression. By providing an in-depth picture of the different modelling techniques, we also aim to assist researchers who seek to build and develop their own models and the associated inference frameworks. Our article thus strikes a unique balance. On the one hand, we provide a comprehensive overview of the available modelling techniques and their applications, including key mathematical expressions. On the other hand, the content is accessible to mathematicians and biomedical scientists alike to accommodate the interdisciplinary nature of cancer research.

# 1. Introduction

Glioblastoma (GBM) is a malignant hierarchically organized brain cancer. It is both the most common and most aggressive type of primary brain cancer in adults [1]. Not only does the diffusive invasion of glioma cancer cells into healthy tissue impede complete resection, but also GBM harbours a sub-population of highly therapy-resistant stem-like cells [2]. Tumour recurrence is inevitable, resulting in a median survival time of 15 months for patients despite maximal treatment [3]. The current gold standard of treatment is the Stupp protocol, which consists of maximal safe surgical resection, followed by radiotherapy and chemotherapy with temozolomide, an alkylating agent [4,5].

Mathematical cancer models have provided a deeper understanding of this immensely complex disease by unveiling the underlying mechanisms and offering quantitative insights [6–9]. Such models have entered all areas of GBM research, ranging from the classification and detection of brain tumours to therapy [10,11].

This review provides the reader with an overview of existing mathematical and computational models that aim to simulate spatially resolved tumour growth. We discuss three main paradigms that have emerged for such *in silico* experiments. In §2, we introduce the so-called continuum models that treat variables, such as the tumour cell density, as continuous macroscopic quantities based on conservation laws. Alternatively, one might represent each cell as an individual agent. Such discrete models are discussed in §3. Section 4 deals with hybrid multi-scale and multi-resolution models that merge and bridge different approaches.

Each of the three methods has its advantages and shortcomings. One must choose between them based on computational limitations and the level of detail required to answer the research questions of interest. With this review, we aim to assist researchers in choosing between the different methods by highlighting the drawbacks and assets of each approach and by showing how the different methods can complement each other. Moreover, we summarize the main concepts and the key mathematical expressions that lie at the core of each approach. We hereby aim to strike a balance between providing a brief overview and showing the mathematics involved. In contrast, many other recent reviews of cancer modelling limit the mathematical details in favour of providing a very concise overview of the literature [12–14].

Mathematical models of GBM draw on a wide variety of molecular and imaging data: histopathological data, computerized tomography (CT), positron emission tomography (PET), single-photon emission computerized tomography (SPECT) and magnetic resonance imaging (MRI), such as T1 weighted (+/– gadolinium contrast), T2 weighted, T2-FLAIR, diffusion-weighted imaging, and most recently spatial and single-cell transcriptomics. The models have thus been employed to shed light on patient-specific data *in vivo* and *ex vivo*, as well as on data from animal models and *in vitro* experiments. These analyses have provided invaluable insights and deepened our understanding of glioma on molecular and structural levels. We address this issue in more detail in §5. The section also discusses the computational challenges posed by systematic inference of model parameters. Finally, §§6 and 7 provide a short overview of some clinical applications of these models and an overall summary, respectively. By including the topics addressed in §§5 and 6, we give our article a more holistic scope with which we aim to set our article apart from other recent reviews on cancer modelling.

While we discuss the different methods in light of GBM, we note that the same models are applied to other types of cancers. Indeed, the models build on concepts that are broadly used to study tissues. Therefore, we not only cite sources that deal with GBM but also occasionally refer the reader to illustrative papers from other areas of oncology and biology [15,16]. It is worth noting that the models are, in a broader sense, actually widely used across scientific disciplines. Throughout the article, we thus present ideas and concepts that are also employed in other fields, ranging from statistical mechanics to solid-state physics. For instance, the cellular Potts model (CPM) presented in §3.1.3 builds on the so-called Ising model used to describe ferromagnetism. We hence encourage the reader to ‘think outside the box’ when exploring the literature, and, in this spirit, we provide a few citations to areas outside the realm of biology.

Before commencing, we would like to point the reader towards other reviews and papers for further details. Lowengrub *et al.* [17] provide a detailed account of continuum models. For an elaborate discussion on discrete models, we refer the reader to Van Liedekerke *et al.* [18]. Both Metzcar *et al.* [12] and Weerasinghe *et al.* [13] give a brief overview of the topic and include a list of recent references. For insights into hybrid multi-scale modelling, we recommend Deisboeck *et al.* [19], and Chamseddine and Rejniak [20]. Falco *et al.* [21] present a concise overview highlighting their clinical implications. Ellis *et al.* [22] focus on mathematical models that address intratumour heterogeneity and tumour recurrence based on next-generation sequencing techniques. Alfonso *et al.* [23] highlight the challenges that mathematical models face when dealing with glioma invasion. Finally, for an overview

of the biology of the GBM from a clinical perspective, we refer the reader to the recent reviews by Finch *et al.* [11] and McKinnon *et al.* [24].

## 2. Continuum models

When dealing with cancer treatment, we face questions related to tumour size, shape and composition. These questions all address cancer on a *macroscopic* scale. While macroscopic tumour dynamics emerge from interactions on a cellular level, it is possible to construct informative mathematical models without tracking individual cancer cells. Instead, the tumour and its environment can be represented as continuous variables that are governed by partial differential equations (PDEs). Such continuum models capture many aspects of cancer *in vitro*, *in vivo* and in patients. They can account for the impact of heterogeneous brain tissue on tumour growth, for different invasive tumour morphologies and, to some extent, even for potential tumour recurrence [25,26]. Moreover, they have successfully been applied in studies on the impact of chemotherapy and repeated immunosuppression treatment [27,28]. Continuum models have thus been employed in diagnosis and treatment planning based on patient-specific data [29–33].

However, PDEs smooth out small-scale fluctuations, which implies that continuum models do not apply to small cell populations, such as those found in the tumour margin. For such small cell numbers, stochastic events play a crucial role, and the applicability and predictive power of continuum models are limited. To properly understand cancer invasion, we must track individual cells. But to do so comes at a high or currently insurmountable computational cost (see §3). Thus, the use of continuum models represents a trade-off that enables and supports scalability and mathematical insights. As a result, continuum models are widely used in the community [13,17,34].

This section introduces the basic mathematical concepts of continuum models and their biological motivation. Any such model in the literature builds on reaction–diffusion equations, describing variables such as the tumour cell density, tumour volume fraction, nutrient (oxygen, glucose) concentration, neovasculature, enzyme concentration, or other properties of the extracellular matrix (ECM) [28,35–38]. Considering any such variable,  $\psi(\mathbf{x}, t)$ , which is a function of position  $\mathbf{x}$  and time  $t$ , we have for its rate of change with time

$$\frac{\partial \psi}{\partial t} = -\nabla \cdot \mathbf{J} + S, \quad (2.1)$$

where  $\mathbf{J}$  is the flux of the considered variable, and  $S$  is the sources and sinks for this variable. Thus, equation (2.1) constitutes a conservation law. The exact expression for  $\mathbf{J}$  and  $S$ , as well as the boundary conditions, will depend on the variable in question. For instance, when dealing with the quasi-steady diffusion of nutrients, equation (2.1) generally takes the following form [39–43]:

$$0 = D\nabla^2 n + S. \quad (2.2)$$

Here,  $D$  denotes a diffusion coefficient, while  $n(\mathbf{x})$  is the relevant nutrient concentration at the location  $\mathbf{x}$  within the considered  $n$ -dimensional domain, which is often denoted by  $\Omega$ .

Alternatively, let's consider the (normalized) cancer cell density,  $\rho(\mathbf{x}, t)$ , at a time  $t$  and location  $\mathbf{x}$ . Many authors assume that the diffusion of cancer cells can be well approximated by Fick's first law

$$\mathbf{J} = -D\nabla \rho, \quad (2.3)$$

where  $D$  denotes a diffusion coefficient, which we discuss in detail in §2.1. As regards the sources and sinks of the cancer cell density, it is commonly assumed that cell proliferation, i.e. tumour growth, is well described by a logistic growth term [44,45]. So, equation (2.1) takes the following form:

$$\frac{\partial \rho}{\partial t} = \nabla \cdot (D\nabla \rho) + \lambda\rho(1 - \rho), \quad (2.4)$$

where  $\lambda$  is the growth rate of the tumour cell population. Other authors assume exponential tumour growth, substituting the second term on the right-hand side by  $\lambda\rho$  [29]. Of course, more than one term might be necessary to summarize the relevant sources and sinks. Several more complex terms are needed, for instance, when considering differentiation between different interdependent tumour sub-populations (cf. §2.2).

It is worth stressing that equation (2.1) cannot stand on its own. Other relations and constraints, including (Neumann) boundary conditions, are needed. One might, for instance, naturally require that

there is no flux at the boundary of the brain domain, i.e. that the tumour does not penetrate the patient's skull [45–47]. This being said, equation (2.1) is the backbone of any continuum model that spatially resolves the tumour (see also §4.1.1).

While we focus on spatio-temporal cancer models in this review, it is worth noting that equation (2.1) can be seen as a natural extension to non-spatial models for tumour growth. Indeed, if we drop any spatial dependence in equation (2.1), including the diffusion term, we end up with an ordinary differential equation (ODE) for the tumour cell density of the form

$$\frac{d\rho}{dt} = S. \quad (2.5)$$

Depending on the source term,  $S$ , equation (2.5) might describe exponential, logistic or Gompertz tumour growth laws that serve as the foundation for non-spatial cancer models. Building on equation (2.5), one might thus construct a sophisticated network of coupled ODEs (or delay differential equations) that might differentiate between different tumour cell sub-populations, or account for immune responses or the effect of cancer treatment (e.g. [48–51] and the references therein). Non-spatial ODEs are thus widely used in mathematical oncology [52]. While such models do not spatially resolve the tumour, they have successfully been used to study the response to drugs and radiation treatments, recovering experimental constraints on the overall growth pattern [53,54]. Here, however, we only intend to mention equation (2.5) in passing to put equation (2.1) into perspective; any further exploration of non-spatial models lies beyond the scope of this review.

## 2.1. Anisotropic diffusion

By using a scalar for the diffusion coefficient in equation (2.4), we assume isotropic tumour growth. However, GBM spreads anisotropically, primarily expanding along pre-existing structures, such as blood vessels and white matter tracks [55–61]. To take the heterogeneous structure of the brain into account, Swanson *et al.* [29] hence proposed to adopt different values for the diffusion coefficients in grey and white matter. Concretely, on the basis of CT scans by Tracqui *et al.* [62], Swanson *et al.* [29] found the diffusion coefficient in white matter to be more than five times larger than in grey matter.

Taking the idea of heterogeneous diffusion further by including anisotropy, other authors [47,58,63–65] substitute the diffusion coefficient with an  $n$ -dimensional diffusion tensor,  $D(\mathbf{x}, t) \in \mathbb{R}^{n \times n}$ . To evaluate  $D(\mathbf{x}, t)$ , Painter and Hillen [47] deploy diffusion tensor imaging (DTI) data. DTI is an MRI technique that measures the anisotropic diffusion of water molecules and hereby maps highly structured tissue. This technique provides the diffusion tensor for water molecules,  $D_{II}(\mathbf{x}, t)$ , throughout the brain. Of course, due to the size difference, the movement of cancer cells is more restricted than that of water molecules, which means that  $D_{II}(\mathbf{x}, t)$  does not adequately describe glioma growth, i.e.  $D(\mathbf{x}, t) \neq D_{II}(\mathbf{x}, t)$ . However, on the basis of a transport equation for individual cell movement, Painter and Hillen [47] establish a relation between  $D(\mathbf{x}, t)$  and  $D_{II}(\mathbf{x}, t)$  expressed in terms of the fractional anisotropy that is commonly used to quantify DTI data [66]. They do so based on a set of simplifying assumptions and parabolic scaling to a macroscopic model (see [67] for further details). Their final macroscopic model takes the following form:

$$\frac{\partial \rho}{\partial t} = \nabla \nabla : (D\rho) + \lambda\rho(1 - \rho), \quad (2.6)$$

where the colon denotes a contraction [26]. The diffusion tensor  $D \in \mathbb{R}^{n \times n}$  is symmetric and positive-definite, as it is related to the variance-covariance matrix of the probability distribution function that describes the velocity changes of individual cells [47,67]. In other words, when dealing with three-dimension data,  $D(\mathbf{x}, t)$  is a symmetric and positive-definite  $3 \times 3$  matrix that incorporates the impact of the local environment on cell migration. The model by Painter and Hillen [47] has been extended and applied by other authors [26,68,69].

Note that equation (2.6) is subtly different from equation (2.4). Apart from  $D$  denoting an  $n \times n$  tensor rather than a scalar, equation (2.6) includes an additional advective-type term since  $\nabla \nabla : (D\rho) = \nabla \cdot (D\nabla \rho) + \nabla \cdot ((\nabla^T D)\rho)$  [26]. Models of the form of equation (2.6) are referred to as Fokker–Planck models, while equation (2.4) is an example of a Fickian model. The additional advection term of the Fokker–Planck model has a demonstrable impact on the solution [70]. We also note that equation (2.6) would correspond to the Fisher's equation if the first term on the right-hand side was substituted by  $D\nabla^2 \rho$ . Indeed, some authors employ a diffusion term of this kind to describe the cancer cell density [71].

## 2.2. Mechanical interactions, cell types, lineage and feedback

Tumours are hierarchically organized. GBMs harbour stem-like cells (GSCs) as well as proliferating (GCP) and differentiating (GTP) sub-populations (cf. [2,61,72,73]). Since these three cell types exhibit very different behaviours, it is insightful to differentiate between these sub-populations, even when dealing with continuum models.

Models that distinguish between viable and necrotic tumour tissue are the first step in this direction. Examples of such models can be found in the papers by Wise *et al.* [74,75] and Frieboes *et al.* [76,77]. Their work is based on reaction–diffusion equations of the form

$$\frac{\partial \rho_i}{\partial t} + \nabla \cdot (\mathbf{u}_i \rho_i) = -\nabla \cdot \mathbf{J}_{\text{mec},i} + S_i, \quad (2.7)$$

where the index  $i$  runs over all sub-populations,  $\mathbf{u}_i$  denotes the velocity of the considered cell species and  $\mathbf{J}_{\text{mec},i}$  is the flux that arises from mechanical interactions as follows:

$$\mathbf{J}_{\text{mec},i} = \mathbf{J}_i - \rho_i \mathbf{u}_i. \quad (2.8)$$

Note that while equation (2.7) appears to differ from the other reaction–diffusion equations listed earlier, this is merely a matter of notation. It is a Fickian model that can be derived by inserting equations (2.3) and (2.8) into equation (2.1). The advantage of phrasing the problem in this manner is that the mechanical flux reflects the mechanical interaction energy that can be obtained from an understanding of the underlying cell biology (see also [25,78–80]). By introducing  $\mathbf{J}_{\text{mec},i}$  it is thus possible to inform the model about the properties of the tumour and host without the need to construct a suitable diffusion tensor.

In articles that employ equation (2.8),  $\mathbf{u}_i$  is computed by imposing relations similar to Darcy's law that links the velocity to a gradient in pressure [25]. For glioma, the relevant expression often takes the form  $\mathbf{u}_i = -\nabla p + \mathbf{F}_i$ , where  $p$  is the solid pressure arising from the tumour proliferation, while  $\mathbf{F}_i$  reflects mechanical interactions.

We exemplify the source functions that enter equation (2.7) by listing the relevant terms for the necrotic tissue according to Wise *et al.* [74], for which

$$S_d = \lambda_A \rho_v + \lambda_N \mathcal{H}(n_N - n) \rho_v - \lambda_C \rho_d. \quad (2.9)$$

Here, the indices 'd' and 'v' refer to the dead and viable cancer cells, respectively, while  $\lambda_A$ ,  $\lambda_N$  and  $\lambda_C$  denote the rates of apoptosis, necrosis and the clearance of dead cells, respectively. Moreover,  $\mathcal{H}$  is a Heaviside step function and  $n_N$  is a viability limit for the nutrient concentration below which cells die—biologically speaking, this term encodes cell death through starvation and the use of the Heaviside step function is a simplifying assumption. For comparison, the source function for the viable tissue takes a similar form:

$$S_v = -\lambda_A \rho_v - \lambda_N \mathcal{H}(n_N - n) \rho_v + \lambda_M \frac{n}{n_\infty} \rho_v, \quad (2.10)$$

where  $\lambda_M$  denotes the rate of mitosis and  $n_\infty$  is the far-field nutrient level.

By distinguishing between GSCs, GCPs and GTPs, Kunche *et al.* [81] and Yan *et al.* [82–84] have incorporated the GBM lineage and hereby taken the discussed models one step further. Kunche *et al.* [81] use this to investigate feedback regulation of cell lineage progression. Furthermore, while previous articles only consider adhesion when computing the mechanical interactions, Chen *et al.* [85–87] include the impact of elastic membranes and the implications of the calcification of dead tumour cells.

## 2.3. Modelling the macroscopic environment

Understanding the microenvironment is essential for understanding GBM since the brain region and other properties, such as the patient's age, have been shown to play a key role in tumour development and heterogeneity [61,88].

The concentrations of different chemicals, including (but not limited to) nutrients, drugs, matrix-degrading enzymes and ECM macromolecules, are commonly modelled using reaction–diffusion equations. The associated diffusion is often in the form  $D\nabla^2\psi$ , but other second-order spatial derivatives can be found in the literature [89–91]. The source terms reflect the processes at play. For instance, the rate of oxygen consumption is often assumed to be proportional to the local oxygen concentration and might be proportional to the local cell density.

Overall, the use of continuum models to model, say, nutrient flows is justified through the different scales that define cancer. Continuum models reliably capture the spatial gradients and temporal variation of nutrients in a way that allows us to assess the behaviour of tumour cells. For some purposes, it might even be adequate to assume that the nutrient levels stay constant over time since cell proliferation takes place on a much longer time scale than nutrient diffusion (cf. equation (2.2)).

Initially, tumours do not possess their own vasculature but rather rely on the diffusion of nutrients and waste products. During this so-called avascular phase, the tumour may lack some features of malignancy and appear more benign. But beyond a certain size (1–3 mm in radius), the nutrient inflow can no longer sustain the growing cell population [92]. Hypoxia, i.e. oxygen shortage, sets in. Without stimulating angiogenesis, i.e. recruiting vasculature, tumour growth will stagnate. However, in response to the hypoxic conditions, the cancer cells release tumour angiogenic factors (TAFs), which stimulates the migration and proliferation of endothelial cells (ECs). New blood vessels sprout towards the tumour, and tumour growth resumes. Understanding the transition from avascular to vascular tumour growth is essential since it is a critical step towards malignancy. To study angiogenesis, many authors model both the diffusion of TAFs and ECs using reaction–diffusion equations [17,30,92–96]. As regards the ECs, we again encounter logistic or exponential source terms. Meanwhile, the gradient of the TAF concentration and that of adhesive molecules (e.g. fibronectin) enter through a flux term encapsulating chemotaxis and haptotaxis:

$$\mathbf{J} = -D\nabla\rho_{\text{EC}} + \sum_i \chi_i\rho_{\text{EC}}\nabla c_i, \quad (2.11)$$

where  $\rho_{\text{EC}}$  denotes the EC cell density and the sum runs over all relevant diffusive components, including TAFs. The concentration of and sensitivity to the  $i$ th components are denoted as  $c_i$  and  $\chi_i$ , respectively [92].

Like continuum models for tumour cells, continuum models for ECs cannot capture the behaviour of individual cells. Some authors, therefore, rely on agent-based models to study the ECs during angiogenesis [97–101]. We refer to §3 for a detailed discussion of agent-based models [102]. Table 1 summarizes the properties of all continuum models discussed in this section.

### 3. Discrete (agent-based) models

Continuum models are based on the assumption that the behaviour of tumour cells is well approximated by macroscopic averages. However, this assumption breaks down for small cell populations since stochastic events dominate these. Therefore, continuum models cannot reliably capture the onset of tumour growth and they do not give a complete picture of the invasive tumour front or margin, i.e. the tumour–host interface, where the cancer cell density is low—although it is possible to address this drawback by linking different scales, as shown by Trucu *et al.* [103] (see also §4). Due to the aggressive invasion of healthy tissue by GBM, this shortcoming is especially problematic for understanding brain tumours. Moreover, continuum models cannot adequately deal with heterogeneity among cells of the same type. To address these issues, one needs to model cancer on a mesoscopic scale following individual tumour cells or cell clusters [104]. Mathematical models that do so are referred to by various names: discrete models, agent-based models, individual-based models or cell-based models. In all cases, cells or cell clusters are modelled as autonomous agents that follow a set of (stochastic) rules prescribing cell movement, death, division and growth. By doing so, discrete models capture the variability among cells that might, for instance, arise as a response to the microenvironment [89]. Note that while discrete models treat cells as autonomous quantities, continuum models are commonly used to depict the microenvironment (cf. §4.1). PDEs hence still come into play when dealing with, e.g., nutrient and drug concentrations [17,105].

Discrete models that describe spatial tumour growth or other cell populations, such as ECs (cf. §2.3), fall into two categories: lattice-based and off-lattice methods. While the former operates on a fixed lattice, the latter does not impose the same restrictions. Lattice-based models can be divided into three sub-categories [12,18]. Firstly, there exists a group of the so-called cellular automata (CA) models that treat all processes, including cell movement, as stochastic processes (cf. §3.1.1). For these models, each lattice site (e.g. pixel or voxel) can be occupied by at most either a single cell or a population of a limited size [106–109]. Each cell or cell cluster is thus characterized by its position on the grid. Secondly, there exist so-called lattice gas cellular automata (LGCA). While these models consider single cells and are conceptually very similar, they differ from other CA models by attributing a

**Table 1.** Overview of the reviewed continuum models. The references are not exhaustive.

model type	features	references
continuum model (CM), tumour	<p><i>Concept:</i> The tumour cell density can be modelled as a fluid using PDEs based on conservation laws.</p> <p><i>Assets:</i> CMs capture macroscopic tumour growth at low computational cost and simple models are analytically tractable.</p> <p><i>Drawbacks:</i> They cannot capture the behaviour at low cell densities (e.g. at the tumour front).</p>	<p><i>Methods:</i> Anisotropic diffusion tensor [26,47,68], cf. S2.1. Interaction energy-based models [25,74,84,87] accounting for lineage [82], cf. S2.2. <i>Patient-specific studies:</i> [30,32,33].</p>
CM, microenvironment	<p><i>Concept:</i> Different properties of the environment, such as nutrient flow or vasculature, are modelled on a macroscopic scale.</p> <p><i>Assets:</i> They are computed at a low computational cost and can be analytically tractable; spatial gradients and time variations, e.g. in nutrient levels, are sufficiently well resolved to study tumour cells.</p> <p><i>Drawbacks:</i> CMs of ECs do not capture the behaviour of individual cells.</p>	<p><i>Nutrient flow:</i> [89–91].</p> <p><i>Vasculature:</i> [17,92].</p> <p>These models are widely used whether the tumour is represented by a CM or by agent-based models (cf. S53 and 4).</p>

velocity to each cell (cf. §3.1.2). After accounting for stochastic events, these models thus include a deterministic evaluation of cell propagation at every time-step. Thirdly, there are so-called CPMs that phrase cell interactions using concepts from statistical mechanics (cf. §3.1.3). CPMs attribute several lattice points to each cell, whereby these models capture cell morphologies. Off-lattice models, also known as lattice-free models, come in two flavours. Centre-based models (CBMs) describe cells as simple particles whose interactions can be expressed as physical forces. Deformable cell models (DCMs) or vertex models (VMs) extend this picture by resolving the cells using several nodes. Like CPMs, DCMs can thereby account for cell morphologies.

One drawback of discrete models is their relatively high computational expense due to the large number of cells that typically need to be simulated. After all, tumours reach  $10^5$ – $10^6$  cells per  $\text{mm}^3$ . However, one benefit of discrete models is their ability to capture emergent properties. The simple rules that govern the (nonlinear) interactions between individual agents will naturally give rise to the dynamics of macroscopic tumour growth. As discussed in §3.1.2, reaction–diffusion equations might thus naturally follow from up-scaling agent-based models [110–113]. Due to the ability of discrete models to capture emergent properties, agent-based models can be calibrated based on patient-specific data and used to predict macroscopic parameters [114,115].

Concerning the implementation of discrete models, it is worth mentioning that some software tools are publicly available. There is no need for a research group to start from scratch. Examples of open-source tools include CHASTE [116], PHYSICELL [117] and COMPUCELL3D [118]. For a recent overview of open-source toolkits, we kindly refer the reader to table 1 in the article by Metzcar *et al.* [12]. In this connection, we note that one must always select and adapt the numerical approach based on the problem at hand. For instance, not all problems require the same geometry. While colon cancer cells and cells *in vitro* move in two dimensions, GBM tumour growth *in vivo* is intrinsically three dimensional, which affects the growth pattern [119]. In the following two sections, we will discuss lattice-based models in more depth (§3.1) and then turn to a detailed discussion of off-lattice models (§3.2).

### 3.1. Lattice-based models

In lattice-based models, we follow a population of cells on a rigid grid. If a regular (e.g. Cartesian) lattice is chosen, artefacts in the established tumour growth pattern might arise, reflecting the lattice symmetries [18]. While unstructured meshes are harder to implement and combine with existing PDE solvers, they do not suffer from this shortcoming [120].

#### 3.1.1. Cellular automata with one or several cells per lattice site

In this section, we discuss two types of CA models: those with at most one and those with multiple cells per lattice site. Both approaches have their advantages and drawbacks. Below, we will start by discussing the single-cell CA models and then continue to frameworks that include many cells per lattice site.

When considering single tumour cells, we follow each of these through a sequence of time-steps. During every time-step ( $t \rightarrow t + \Delta t$ ), a cell might migrate to a neighbouring lattice site, it might die, it might divide or it might grow, whereby it temporally occupies two sites before dividing. All of these events can be modelled as stochastic processes or be imposed through deterministic conditional statements that encompass our knowledge about cancer—additional parameters, such as age, mutation or phenotype, might be included in these rules [121]. For instance, while cells might die spontaneously, external factors can make cell death increasingly likely. Thus, tumours develop a necrotic core due to nutrient deprivation. One might, therefore, set the probability for individual cell death to depend on the distance to the tumour front [109], the local nutrient concentration or the local level of toxic metabolites [108].

Tumour cell migration is also affected by the location of the cell within the tumour. If we consider a cell that is deeply buried within the tumour, all surrounding lattice sites are already occupied and there is nowhere to migrate. This notion also plays a role in cell proliferation. To divide, a cell deep within the tumour must push its neighbours away to make space for the daughter cell, which becomes increasingly difficult as the distance to the tumour edge increases. For simplicity, many authors account for this notion by introducing a sharp cut-off: if there are no free sites within a certain distance, the cell will be unable to divide [122]. Other models assume a smooth decline in proliferation with depth [112,123]. On a macroscopic level, this suppression of cell division leads to a proliferative rim of constant width, below which we encounter a quiescent cell population surrounding a hypoxic region with a necrotic core at its centre. In accordance with data, this model



predicts that a tumour spheroid enters linear growth after initially growing exponentially [124]. As regards cell division, we also note that experiments suggest that the cell cycle time follows a  $T$ -like distribution, e.g. an Erlang distribution [125]. The rules imposed on the individual cells can account for a broad range of cell properties. For instance, if the CA model accounts for the hierarchical nature of tumour cells (GSCs, GCPs and GTPs), the probability of cell proliferation will also depend on the attributed cell type [121].

When solving the system numerically, one must choose a suitable time-step,  $\Delta t$ . For this purpose, it is helpful to consider the cell population as a whole. Every time a cell dies, moves, divides or grows, the system as a whole will transition into a new state. The time-step should be chosen accordingly such that only one event is likely to occur within  $\Delta t$ , and thus  $\Delta t$  is itself a function of time. To achieve this, one might distil the temporal dynamics of the system into a master equation and employ kinetic Monte Carlo algorithms [112,126–128]. Moreover, the order in which the individual cells are updated should be random to avoid grid artefacts [17].

Rather than considering individual cells, one might track cell clusters of a limited size, keeping track of the number of cells at each lattice site. The underlying concepts stay the same. The advantage of reducing the resolution in this manner is the reduced computational cost, which allows for modelling tumours of centimetre size [125,129]. Meanwhile, a coarser resolution might lead to artefacts affecting the predicted tumour growth. Another drawback of both single- and multiple-cell CA models is the fact that they do not properly account for cell morphologies. For models that address this issue, see §3.1.3.

### 3.1.2. Lattice gas cellular automata models

Like the models in §3.1.1, LGCA models follow a set of stochastic rules to determine whether individual cells die, grow or divide. But in addition to specifying the location of the cells on the lattice, LGCA models attribute a discrete set of velocity channels to each spatial location. Hence, the cells roam a discretized phase space.

Analogously to migration in the CA models presented earlier, cells might stochastically migrate in phase space: they can move to neighbouring *velocity channels* following probabilistic rules. At most, one cell can occupy any given velocity channel at a given location. This restriction is not to say that these channels are unique, i.e. at each location there might be one or more channels with the same velocity, including channels at which the cell is at rest.

When using LGCA models, the time evolution of the system is split into two distinct steps. Firstly, the model allows for a number of stochastic events that correspond to the number of cells—they can die, grow, divide or change velocity channel. Afterwards, the model updates the position of every cell based on its individual velocity complying with momentum and mass conservation. In this manner, the model alternates between accounting for probabilistic interactions and deterministic cell movement. These basic concepts of LGCA models are summarized in figure 1.

Within the mean-field approximation, Hatzikirou and Deutsch [110] show that the Boltzmann equation governs the macroscopic dynamics of LGCA models. (The Boltzmann equation can be used to describe the evolution of thermodynamic systems that are out of equilibrium. Applications range from quantum mechanics over cosmology to MRI [130].) Furthermore, through Taylor expansions and scaling, they arrive at a reaction–diffusion equation with a logistic growth term, giving a microscopic justification for the success of the models presented in §2.

LGCA models offer an intuitive implementation of cell migration. By comparing model predictions to experimental data, several studies have thus used such models to gain insights into cell–cell interactions and mechanisms that underlie tumour invasion [111,131,132]. In particular, the cited articles focus on the so-called ‘Go or Grow’ (GoG) hypothesis. This hypothesis addresses the fact that glioma cells exhibit an inverse correlation between cell migration and proliferation [133]. It states that migration and proliferation are mutually exclusive events, i.e. that moving cells cannot divide. This dichotomy stems from shared signalling pathways [134]. Since the transition from benign to malignant tumour growth is coupled with a transition from a highly proliferative to a highly migrative phenotype, it is paramount to understand the link between these two phenomena. Specifically, Monteiro *et al.* investigate the role of hypoxia [135].

### 3.1.3. Cellular Potts models

CPMs define a Hamiltonian function,  $H$ , to incorporate cell movement and growth, interactions between adjacent cells, and interactions between cells and their microenvironment (see [136] for a detailed

LGCA models

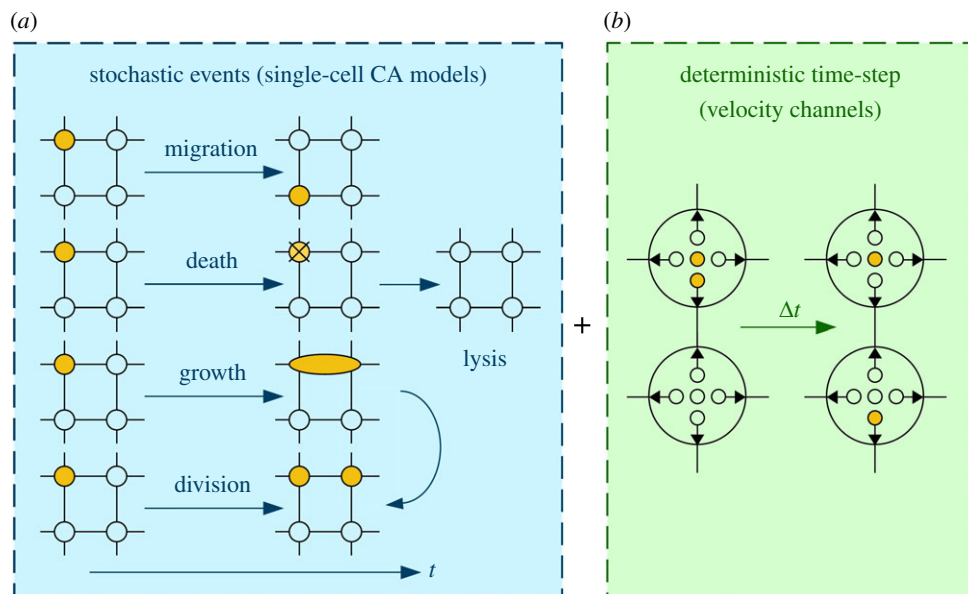


**Figure 1.** Schematic overview of the concepts behind LGCA models. (a) The cell dynamics that are handled as stochastic processes in the single-cell CA models discussed in §3.1.1: cell migration, death (and lysis), growth and cell division. Filled (orange) circles denote occupied sites, while there are no cells in the empty circles. (b) LGCA models attribute a set of velocity channels to each location, subdividing each site. The cells can shift between these channels following stochastic rules. Again, filled (orange) circles denote occupied channels, while empty channels are indicated by empty circles. Here, there are five velocity channels per location: four channels that lead to migration and one channel at which the cell is at rest. For LGCA models, the time evolution takes place in two steps. First, cell death, growth, division and migration between *velocity channels* occur as stochastic events. Cell migration between lattice sites, however, is no longer included in this step. Instead, cell migration takes place in the second step based on the velocity channels that the cells occupy. In this second step, cell migration complies with momentum and mass conservation.

0	1	1	1	0	0	0	0	0	0
1	1	1	1	1	*	2	0	0	0
0	1	1	1	*	2	2	2	0	0
0	*	1	2	2	2	2	2	0	0
0	0	0	2	2	2	2	2	0	0
0	0	0	0	2	0	0	0	3	0
0	0	0	0	0	0	3	3	3	3
0	0	0	0	0	*	3	3	3	3
0	0	0	0	0	0	3	3	3	0

**Figure 2.** Schematic overview of CPMs. Each cell (and the ECM) has a unique identifier. Here, we consider cells 1, 2 and 3 and the ECM denoted by 0. Each cell occupies several lattice sites. Randomly selected sites at the cell borders (asterisks) might swap affiliation depending on the energy change associated with this swap, allowing the cells to grow and move.

discussion of Hamiltonian mechanics). Moreover, CPMs attribute multiple lattice sites to each cell, which allows the models to account for cell morphology. Again, CPMs do so via the Hamiltonian function. The basic concepts are illustrated in figure 2.

For simplicity, let's consider a Hamiltonian of the following form [97,137]:

$$H = \sum_{(\mathbf{x}, \mathbf{x}')} E(\tau(\sigma(\mathbf{x})), \tau(\sigma(\mathbf{x}')))(1 - \delta(\sigma(\mathbf{x}), \sigma(\mathbf{x}'))) + \lambda_V \sum_{\sigma} (V(\sigma) - V_T)^2. \quad (3.1)$$

The first term on the right-hand side of equation (3.1) summarizes the contact energy at the cell interfaces. The sum runs over all pairs of adjacent lattice sites ( $\mathbf{x}, \mathbf{x}'$ ). Each cell (and the ECM) has a unique identifier  $\sigma$ , i.e. lattice sites with the same value of  $\sigma$  are associated with the same cell (or the ECM). Moreover, each cell has a type  $\tau$  (e.g. GSC, GCP or GTP; see [138]).  $E(\tau(\sigma(\mathbf{x})), \tau(\sigma(\mathbf{x}')))$  denotes the contact energy per unit surface area (in 3D) between a cell of type  $\tau(\sigma(\mathbf{x}))$  and a cell of type  $\tau(\sigma(\mathbf{x}'))$ . The Kronecker delta,  $\delta(\sigma(\mathbf{x}), \sigma(\mathbf{x}'))$ , is needed since we only encounter an interface if  $\sigma(\mathbf{x}) \neq \sigma(\mathbf{x}')$ , while there will be a contact energy associated with cells of the same type. The second term on the right-hand side of equation (3.1) represents a penalty for deviations between the volume,  $V(\sigma)$ , of a cell and its target size,  $V_T$ . Here, the sum runs over all cells.

At every time-step, the CPM selects a random set of lattice sites at the cell boundaries and attempts to overwrite their cell affiliations ( $\sigma$ ) with those of neighbouring sites:  $\sigma(\mathbf{x}) \rightarrow \sigma(\mathbf{x}')$ . In this manner, cells grow and move by hijacking adjacent sites, whereby they might have to push other cells aside. Whether these proliferation and growth attempts are successful or not is decided by a Metropolis algorithm based on the associated change in the Hamiltonian function (see [139] for a discussion of such algorithms). The proposed change in cell affiliation is accepted with the probability

$$P(\sigma(\mathbf{x}) \rightarrow \sigma(\mathbf{x}')) = \min\left(1, \exp\left(-\frac{\Delta H}{\beta}\right)\right), \quad (3.2)$$

where the motility of the cells increases with the increasing Boltzmann temperature,  $\beta$  (cf. [137]).

One can include additional terms in equation (3.1) to add more information about cell biology. For instance, in analogy to the volume constraint, Ouchi *et al.* [140] suggest including constraints on the surface area of the cell (in 3D) [141]. Other authors include chemotaxis, motility, haptotaxis and haptokinesis in this manner [98,142–146]. One immediate drawback of CPMs is that they are limited to phenomena and cell properties that can be formulated as terms in a Hamiltonian.

Meanwhile, when accounted for, cell division and death are treated as stochastic events or occur when certain conditions are met. For instance, Gao *et al.* [138] let cells attempt division when  $V(\sigma) > 2V_T$  and impose apoptosis for proliferating glioma cells after a pre-determined number of division attempts. Other authors impose (probabilistic) conditions on apoptosis and necrosis based on nutrient levels or overcrowding [97,141].

## 3.2. Off-lattice models

One of the main drawbacks of lattice-based models is that the lattice introduces a lower length scale. Off-lattice models overcome this problem at the expense of increased computational cost. We give a schematic overview of the two different types of off-lattice models in figure 3.

### 3.2.1. Center-based models

CBMs treat cancer cells as physical particles whose trajectories can be deduced from their equations of motion [136]. The cells themselves are usually represented as spheres (in 3D) or viscoelastic ellipsoids that deform when subjected to external forces [147]. During mitosis, the mother cells are often modelled as dumb-bells, consisting of two overlapping spherical cells [148].

The equations of motion can be derived within an energy-based picture or by modelling the relevant interactions as physical forces that act on the particles. In the latter approach, the models draw on Newton's second law and commonly assume that inertial forces and any average acceleration can be neglected (cf. Brownian dynamics). Put another way, we are dealing with friction-dominated overdamped motion, which means that friction forces balance out all the other forces [18,122,124]. For cell  $i$  on a substrate, we can then write (cf. [18])

$$\Gamma_i^{\text{cs}} \frac{d\mathbf{x}_i}{dt} + \sum_{j \neq i} \Gamma_{ji}^{\text{cc}} \left( \frac{d\mathbf{x}_i}{dt} - \frac{d\mathbf{x}_j}{dt} \right) = \mathbf{F}_i^{\text{sub}} + \mathbf{F}_i^{\text{mig}} + \sum_j (\mathbf{F}_{ji}^{\text{adh}} + \mathbf{F}_{ji}^{\text{rep}}). \quad (3.3)$$

The first term on the left-hand side expresses cell–substrate friction forces, while the second term deals with friction between cells. Here,  $\Gamma_{ji}^{\text{cs}}$  and  $\Gamma_{ji}^{\text{cc}}$  are tensors that account for anisotropies and inhomogeneities. For instance, for spherical cells in a homogeneous and isotropic environment,  $\Gamma_{ji}^{\text{cs}} = \gamma \mathbb{1}$ , where  $\gamma$  is a damping coefficient and  $\mathbb{1}$  is the identity matrix [122]. Thus, the drag force that acts on a cell in an isotropic viscous environment is proportional to the cell's velocity [149].

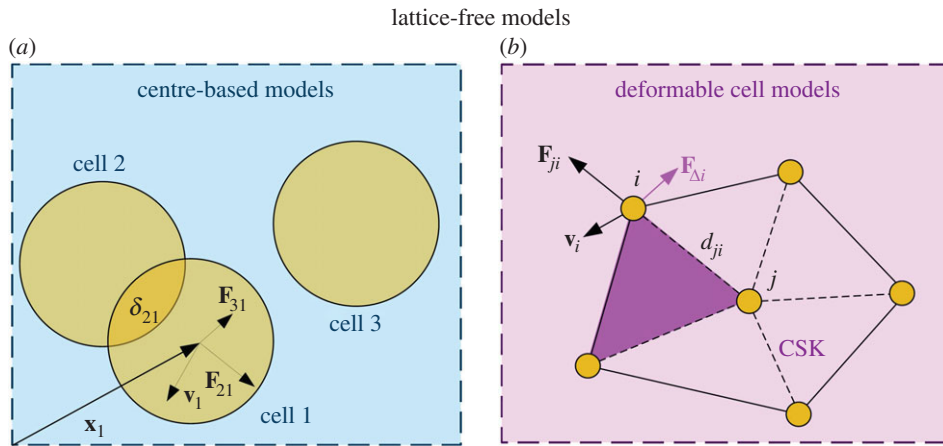


**Figure 3.** Schematic overview of off-lattice models. (a) Spherical cells in a CBM, highlighting forces on cell 1. Due to the overlap ( $\delta_{21}$ ) between cells 1 and 2, cell 1 is repulsed by cell 2. Overlapping cells forming a dumb-bell also occur during cell division.  $F_{31}$  exemplifies an adhesive force occurring without direct contact. In an isotropic environment, the drag force will be proportional to the velocity,  $\mathbf{v}_1$ . (b) A cell made of multiple nodes in a DCM. Node  $i$  at the cell membrane is subject to forces from the surrounding nodes ( $F_{ji}$ ). Constraints on areas and volumes might lead to additional forces ( $F_{\Delta i}$ ), while the movement of the node ( $\mathbf{v}$ ) gives rise to viscous forces. The cell has a cytoskeleton (CSK, dashed lines).

On the right-hand side of equation (3.3),  $F_i^{\text{sub}}$  denotes forces that emerge from adhesion and repulsion between cell  $i$  and the substrate.  $F_i^{\text{mig}}$  describes the migration forces. For instance, chemotaxis might introduce a preferred direction for migration [122]. One might account for the memory of cells, i.e. the persistence of a cell to move in a given direction. Some authors do so using inertial forces. In addition, some authors include cell polarity, giving the cell a preferred direction of motion.  $F_i^{\text{mig}}$  becomes a noise term that describes a random movement in the absence of such forces and assumptions. The last term on the right-hand side summarizes the adhesion and repulsion between cell  $i$  and all other cells. These forces will typically depend upon the distance between the cell centres or the amount of overlap,  $\delta_{ji}$ . Contact mechanics offers different approaches to model these cell–cell interactions, including Hertzian formulations and the Johnson–Kendall–Roberts model of elastic contact (cf. [110,148]). Some authors simply assume that all forces involved in cell–cell interactions are well approximated by linear springs, generalized linear springs or polynomial expressions (e.g. [43,149,150] and the references therein).

To exemplify the use of equation (3.3), let's consider spherical cells, whose movement is dominated by isotropic friction on the substrate and cell–cell interactions. Meineke *et al.* [150] and Drasdo [122] use this model to describe cellular mono-layers in the intestinal crypt and *in vitro*. For mono-layers, we might assume that all cells have roughly the same velocity, which leaves us with the first term on the left-hand side and the last term on the right-hand side of equation (3.3):

$$\gamma \frac{d\mathbf{x}_i}{dt} = \sum_j (F_{ji}^{\text{adh}} + F_{ji}^{\text{rep}}), \quad (3.4)$$

which amounts to a set of coupled ODEs that can be solved using explicit or implicit schemes, such as a forward Euler scheme [149,150]. In general, equation (3.3) can be written as a set of linear equations and be solved using matrix manipulation, for which standard software packages are available.

The computational challenge of CBMs is twofold. Firstly, all interacting cell pairs must be identified. Secondly, the relevant interactions take place on chemical and dynamic time scales that are much shorter than the time scale that governs tumour growths. Besides their high computational cost, it should be noted that CBMs might suffer from artefacts when cells are densely packed [18]. Despite these shortcomings, CBMs have widely and successfully been applied to study tumour-related issues, such as drug response [151,152].

### 3.2.2. Deformable cell (vertex) models

DCMs are conceptually similar to CBMs: cell dynamics are distilled into equations of motion. However, rather than representing each cell by simple geometrical objects, DCMs depict cells as a number of

connected nodes (cf. figure 3). In contrast to CBMs, DCMs hereby capture cell morphology and intracellular mechanics. The nodes within a cell are connected by viscoelastic elements that are part of either the cell membrane or the cytoskeleton. It is essential to include a cytoskeleton since the modelled cells might buckle without an internal scaffolding structure [153].

Assuming that inertial forces can be neglected, the equation of motion for any given node takes the same form as that of a single cell in CBMs (cf. equation (3.3)). Thus, frictional forces balance out all other forces acting on the node (see also [154]). Node–node interactions can be modelled by letting the viscoelastic elements, i.e. parts of the cell membrane or the cytoskeleton, act as damped linear springs. To better depict the behaviour of biopolymers, one might model the elements using nonlinear forces [155,156]. Besides node–node interactions, we must introduce forces that express area and volume constraints on the cell as a whole or on subdivisions spanned by several nodes. By considering subdivisions of the cell membrane, we might furthermore introduce forces that express the resistance of the cortex to bend [156].

Simulating realistic cell dynamics requires a large number of nodes per cell and the models can become rather complex. Due to the resulting high computational cost, it is often only feasible to simulate single cells or small cell populations on short time scales.

For completeness, it should be mentioned that there is a subgroup of DCMs called VMs. In such models, the cells are represented as polygons spanned by a grid of nodes, i.e. adjacent cells share vertices and edges. There is no space between cells. VMs are useful when dealing with densely packed cells and have thus found applications in tissue mechanics but have not been applied to GBM [157–159].

Table 2 gives an overview of all discrete methods discussed earlier.

## 4. Hybrid multi-scale models

In the literature, the term hybrid or multi-scale model might denote any combination of the different methods discussed earlier. A large variety of approaches thus fall into this category. Adopting the nomenclature from Deisboeck *et al.* [19], we distinguish between three types: *composite* hybrid models, *adaptive* hybrid models and calibrated models, such as continuum models with functional parameters. However, we note that the literature generally does not explicitly distinguish between these three types.

Composite hybrid models track and connect phenomena across various scales while keeping the scale associated with each individual aspect fixed (cf. §4.1). Thus, all tumour cells are treated on an equal footing but not in the same way as their environment. Since the coupling between a tumour and its environment must be considered in real-world applications, and since the environment can be modelled using PDEs, the agent-based models discussed in §3 are consequently often referred to as components of composite hybrid models when they are encountered in the literature.

In contrast, adaptive hybrid models dynamically adjust the local resolution based on the required level of detail (cf. §4.2). That is to say that not all tumour cells are represented in the same manner. Finally, the third type of hybrid model denotes, for instance, continuum models, whose parameters have been calibrated based on agent-based models, or biophysical considerations of microscopic or mesoscopic phenomena (cf. §4.3).

### 4.1. Composite hybrid models

When using a discrete model to represent tumour cells, the extracellular biochemical players, such as oxygen, are commonly modelled as continuous fluids [91,164–166]. Moreover, intracellular changes, i.e. processes on a sub-cellular scale, might be tracked for each individual cell using ODEs as discussed in §4.1.1. These different microscopic, mesoscopic and macroscopic mechanisms are all coupled. For instance, the nutrient levels both depend on the cell density and impact the probabilities that are used to predict cell actions. When this interdependence is taken into account, the discrete tumour cell model becomes one of many components in a larger framework that spans and links multiple temporal and spatial scales. The framework as a whole then constitutes a composite hybrid model (cf. [20,65,89,151,167–174]). Such hybrid frameworks have been used to study a wide variety of phenomena, including drug resistance [152,175]. In each case, the focus of the study prescribes the resolution of different features. For instance, in some studies, discrete models of the vasculature are combined with continuum models of the tumour to better understand angiogenesis or drug delivery [101]. As another example, May *et al.* [176] couple discrete tumour models with biomechanical

**Table 2.** Overview of the reviewed discrete models. The references are not exhaustive. For other recent reviews, see [12,13,18,160,161].

model type	features	references
CA model	<p><i>Concept:</i> All CA-type models are discrete and lattice based. Cell migration, death, movement, division and growth are modelled as stochastic processes.</p> <p><i>Particularity:</i> Multiple cells or at most one are allowed per lattice site.</p> <p><i>Assets:</i> Centimetre-scale simulations are feasible when tracking cell clusters. Individual cells can be represented.</p> <p><i>Drawbacks:</i> They do not represent cell morphology, have a limited spatial resolution and are computationally heavy. For multiple cells per site, the individual cell positions are not tracked.</p>	<p><i>One cell per lattice site:</i> [112,121,125,162].</p> <p><i>Multiple cells per lattice site:</i> [107,109].</p> <p><i>Bridging scales:</i> The limit on the number of cells per site (i.e. the resolution) can vary between different locations [18].</p>
LGCA model	<p><i>Concept:</i> They are CA-type models. There are multiple velocity channels (and hence cells) per lattice site. A deterministic step evaluating movement is included (figure 1).</p> <p><i>Assets:</i> Individual cells are represented. Convergence to CM has been shown.</p> <p><i>Drawbacks:</i> They do not represent cell morphology, have a limited spatial resolution and are computationally heavy.</p>	<p>Deutsch, Hatzikirou and collaborators have investigated cell proliferation and glioma invasion [110,111,131,132].</p>
CPM	<p><i>Concept:</i> They are CA-type models. There are multiple sites per cell. A Hamiltonian function governs stochastic events.</p> <p><i>Assets:</i> CPMs draw on the physics behind the cell dynamics and represent cell morphology.</p> <p><i>Drawbacks:</i> They have a limited spatial resolution. Centimetre-scale simulations are not feasible.</p>	<p>Authors have included a broad range of phenomena through a variety of terms in the Hamiltonian [97,98,138,140,143].</p>
CBM	<p><i>Concept:</i> CBMs model cells as physical particles governed by their equations of motion. No lattice is used. Cells are simple geometrical objects.</p> <p><i>Assets:</i> The physics behind the cell dynamics is accounted for. Cells and their movement are resolved.</p> <p><i>Drawbacks:</i> CBMs are computationally heavy. Centimetre-scale simulations are not feasible. Cell morphology is not modelled.</p>	<p>Cells can be spherical [110,148] or ellipsoidal [147]. Studies of tumour cell drug response: [152].</p>
DCM	<p><i>Concept:</i> Cells are depicted as a collection of connected nodes described by their equations of motion.</p> <p><i>Assets:</i> DCMs model cell morphology and stresses on a sub-cellular level. There is no lattice that would impose a limited spatial resolution.</p> <p><i>Drawbacks:</i> Only simulations of small cell populations or single cells are feasible.</p>	<p>Single-cell adhesion and response to mechanical stress [155,156], tumour cell proliferation [163], vertex models [158].</p>

calculations of stresses and strains to arrive at a more accurate prediction of the tumour shape. Finally, we note that composite hybrid models have been employed in Bayesian inferences to establish posterior probability distributions for relevant model parameters [123] (see also §5).

#### 4.1.1. Ordinary differential equations

When dealing with agent-based hybrid models, some authors include sub-cellular dynamics, modelling molecular networks, pathways and reactions [167,168,172,177]. Such processes are governed by a system of coupled nonlinear ODEs that represent mass balance equations and rely on the stoichiometry of the underlying biochemical reactions. If we consider  $N$  molecular species, the rate at which the concentration ( $X_i$ ) of the  $i$ th species changes is thus a function ( $f_i$ ) of the concentrations of the  $N$  different species such that we have a set of coupled differential equations of the following form:

$$\frac{dX_i}{dt} = f_i(X_1, \dots, X_N). \quad (4.1)$$

The right-hand side of equation (4.1) depends on the system in question but typically contains linear terms, quadratic terms, Michaelis–Menten terms or other nonlinear functions such as Hill function terms (see also [178] for an introduction to Michaelis–Menten kinetics). It is beyond the scope of the present paper to go into any further details. Rather, we kindly refer the reader to the references listed at the beginning of this section.

ODEs thus play a vital role in some composite hybrid models. In general, ODEs are a common tool in mathematical biology and oncology. For instance, they can capture global tumour growth patterns as briefly mentioned in §2.

## 4.2. Adaptive hybrid models

Detailed modelling of individual cells is required to capture tumour growth at low cell numbers. Agent-based models thus give unique insights into glioma invasion. However, at high cell densities, a lower resolution suffices. Continuum models realistically capture all relevant aspects of large chunks of bulk tumours. Adaptive hybrid models take advantage of this notion by describing different parts of the tumour tissue using distinct modelling approaches. Thereby, it becomes possible to draw on the strengths of discrete models when depicting centimetre-sized tumours without the insurmountable computational cost that would otherwise be involved.

The hybrid model presented by the groups of Kim and Stolarska [172,179,180] treats necrotic tumour zones, quiescent tumour tissue and the surrounding microenvironment as continuous fluids. The relevant PDEs are solved on a regular grid. The cells in the proliferative tumour rim (100–200  $\mu\text{m}$ ), on the other hand, are modelled using a CBM. They are represented as autonomous ellipsoids. At the boundary between the cell-based and continuum components, interpolation is used to communicate the forces that individual agents exert on the continuous component and vice versa (see also [181] for a related example from molecular dynamics).

Bearer *et al.* [182] and Frieboes *et al.* [183] couple an off-lattice approach with the continuum models by Wise *et al.* [74] discussed in §2.2. To study glioma invasion, they include dynamic transitions between the continuum and cell-based representations based on the microenvironment. In their model, both mutations and hypoxia might induce the development of a migratory phenotype [184].

The adaptive hybrid models discussed earlier allow for mass transfer between the different components and are carefully constructed to obey laws, such as mass conservation. However, it is worth noting that the continuum models are pre-assumed without guaranteeing that the imposed functional form emerges from up-scaling the cell-based representation (cf. §4.3). Moreover, due to the assumptions that enter the continuum and agent-based models, single-cell measurements might lead to different parameter values than those required for continuum models to fit patient-specific data [185].

Rather than coupling agent-based and continuum models, other authors [18,186,187] combine agent-based models with different resolutions. Such approaches are known as multi-scale agent-based modelling. For instance, one might couple CA models that consider single cells with models that deal with cell clusters at a coarser lattice resolution (see also [188] for a multi-resolution study of polymers).

It is an intricate task to couple models that represent the tumour on different scales. After all, the models might rely on very different paradigms—e.g. one might seek to create an interface between a stochastic and a deterministic model. As a result, a variety of approaches can be found in the literature. For a recent review, we refer the reader to the article by Smith and Yates [189]. But as a

final example, it is worth mentioning the article by Yates *et al.* [190] that demonstrates how to construct a transition region where the two models in question coexist with spatially varying contributions to the predicted dynamics.

### 4.3. Calibrated models

Various authors encode information from cell-based models or biophysical considerations into heterogeneous and time-varying parameters of continuum models. This goal can be achieved in different ways. As briefly discussed in §3.1.2, one might up-scale agent-based models using the mean-field approximation (cf. [110]). Other authors draw on the emergent macroscopic properties of agent-based models to derive phenomenological relationships (cf. [17,114]).

Each method mentioned earlier relies on simplifying approximations to derive an analytical expression, which might limit their predictive power. To circumvent the need to explicitly state expressions for the macroscopic variables altogether, Kavousanakis *et al.* [191] use a form of equation-free modelling called coarse projective integration [192]. This method invokes the so-called coarse time-stepper that consists of four phases: lifting, simulation, restriction and extrapolation. These four phases are repeated for every macroscopic time-step. In the lifting step, an ensemble of cell distributions is drawn from the macroscopic tumour cell density. Each cell distribution is then evolved over a short time span using an agent-based model—Kavousanakis *et al.* use a CA model. In the restriction step, the macroscopic density is updated by computing the ensemble average of the agent-based simulations. Under the assumption that the macroscopic cell density evolves more slowly than the microscopic variables, the observed change in the cell density yields an estimate of its time derivative. Using the forward Euler method, this information can be employed to project the cell density further into the future without considering individual cells.

We note that the general idea of calibrating coarse models based on more resolved representations is not only limited to continuum models. Recently, Van Liedekerke *et al.* [193] have thus calibrated the mechanical interaction forces of CBMs based on DCMs.

## 5. Data-driven modelling

Researchers draw on a wide range of experimental data to inform their mathematical models of GBM and do so following several different approaches. One can use data to select the underlying mechanism or inform the model parameters. For example, as discussed earlier, some researchers use DTI MRI data to determine the diffusion properties of cancer cells. Moreover, data allow for qualitative comparisons and constraints on the simulations. For instance, most models are set to recover generic properties of cancer, such as spherical avascular tumour growth. Finally, one can use data to infer model parameter values using a statistical framework, either maximum likelihood estimation or a Bayesian approach. Systematic incorporation of imaging and molecular data into the mathematical models of cancer via statistical inference is a promising and timely area of future development. This area of development is bolstered by the latest progress in imaging and omics approaches, which are producing quantitative data on an unprecedented scale. Furthermore, the latest progress in computational power, simulation-based inference methods and machine learning make this task computationally feasible. Several modelling studies aim to fit specific data from patients, animal models or *in vitro* experiments. Here, we provide a list of illustrative examples and summarize our perspective on important areas of future research. We also refer the reader to some recent reviews on the topic [14,194].

Two decades ago, Stamatakos *et al.* [195,196] used agent-based models to investigate the impact of chemotherapy *in vivo* based on patient-specific PET, SPECT, T1-weighted MRI, histopathologic and genetic data. They reduced the computational cost by clustering the cells into macroscopic ( $1\text{mm}^2$ ) regions rather than simulating individual cells. More recently, Gallaher *et al.* [151] published a study in which they fit MRI and *ex vivo* cell-tracking data from rats to off-lattice agent-based models, simulating individual cells. They accomplish this fit by using random sampling because many fitting algorithms struggle with the stochastic nature of the agent-based models [197,198]. However, due to the high computational cost, agent-based models are most commonly found in studies focusing on small cell populations. For instance, Oraiopoulou *et al.* [199] use agent-based models to recreate the invasive morphologies of GBM observed *in vitro*. Meanwhile, many articles on agent-based models do not include a fit to real-world data but rather perform *in silico* experiments to make qualitative and quantitative predictions. For instance, on the basis of such analyses, Perez-Velazquez and Rejniak



[152] addressed the development of drug resistance, Kim *et al.* [171,172] investigated the key mechanisms behind molecular switches, and Schmitz *et al.* [109] studied growth patterns.

The parameters used in state-of-the-art continuum models [185] to capture the migration and proliferation of GBM are derived from MRI and CT images, and the application of continuum models to patient-specific data *in vivo* is widespread in the literature. Thus, Swanson *et al.* [27,29] already used such data to inform their models 20 years ago [200]. Later studies that build on their work have included further imaging data, such as PET [30,32,201]. Isotropic diffusion reaction equations yield a detailed picture based on T1Gd and T2-FLAIR MRI images [31]. Other studies have employed histopathology [25]. The anisotropic continuum models discussed in §2.1 likewise built on MRI data, drawing on DTI images to compute the diffusion matrix [26,47,63,68,202].

Due to the relatively low computational cost of continuum models, they can be employed in Bayesian sampling schemes as illustrated by Lipkova *et al.* [203], who infer model parameters based on MRI and PET images using a Markov Chain Monte Carlo algorithm. Based on a clinical study conducted on eight patients, Lipkova *et al.* demonstrate that their Bayesian approach can be used to design personalized radiotherapy plans that harm less healthy tissue than the standard treatment protocol while achieving the same efficiency in terms of tumour recurrence within a predefined volume.

Ezhov *et al.* [204] address the same inverse problem using machine learning in tandem with continuum models. Ezhov *et al.* construct a library of 100 000 simulations with different parameter values and use their atlas to train a neural network. The trained neural network can infer the patient-specific model parameters based on MRI images within minutes, allowing for effortless model personalization. Today, continuum models are thus at the point where they have the potential to enter clinical settings and contribute to personalized treatments. While the same does not yet hold for agent-based models due to their high computational cost, machine learning might likewise help to overcome this obstacle in the future, as discussed by Jørgensen *et al.* [198]. Machine-learning algorithms would play the same role as they do in continuum models by circumventing the need to produce further simulations once a surrogate model or inference algorithm has been trained. Similar strategies are applied when dealing with agent-based models outside of cancer research [205].

Like imaging data, molecular data offer unique insights into GBM [206,207]. In particular, different sequencing techniques, including bulk RNA-seq [208], scRNA-seq [209–214] (recently reviewed in [215,216]) and spatial RNA-seq [217], have helped researchers to uncover different aspects of brain tumours. Sequencing data have thus contributed to our understanding of important cell types, the nature of the invasive tumour front, the spatial cellular organization of the tumours and the molecular basis of the heterogeneity of GBM. For instance, Ravi *et al.* [217] recently identified spatially distinct clusters of genes via spatial transcriptomics, and Neftel *et al.* [209] identified four main cellular states among malignant tumour cells by analysing data at the single-cell level. Furthermore, Neftel *et al.* demonstrated that the relative frequency of these four states varies between GBM samples. On the one hand, such information on the heterogeneity of GBM is valuable in its own right and can help to inform the underlying assumptions used in the mathematical models. As exemplified in §2.2, mathematical models thus present a unique tool to investigate the implications of such information on the tumour phenotype. On the other hand, the vast number of spatial GBM sequencing data that is becoming available can directly be used in parameter inference, model selection or validation of model predictions. Thus, mathematical models might be applied to fit the cell-type distributions that spatial GBM sequencing data uncover.

## 6. Clinical application of spatio-temporal modelling in GBM

GBM is a biologically complex and dynamic tumour that exists within the intricate and responsive brain environment. Parcelling and modelling discrete aspects of these biological processes and systems holds the potential for numerous direct clinical care applications and has the potential to address several areas of unmet need.

Mathematical diffusion tensor modelling is currently widely used in the context of MRI diffusion tensor-based tractography for the modelling of white matter tracts. Understanding patient-specific anatomy, and anatomic-pathological relationships, is critical for effective surgical planning and avoidance of iatrogenic injury [218]. Future refinements in data modelling can be expected to improve spatial resolution and reliability, which would directly translate to improved validity of neuro-imaging with direct clinical applications—as exemplified in the study by Lipkova *et al.* discussed in §5.

**Table 3.** Overview of how different model types can deal with properties that define GBM growth.

phenomenon	continuum models	agent-based models
invasion of healthy tissue	diffusion (and advection) terms are included in the PDE.	stochastic (and deterministic) rules dictate the migration of individual cells.
anisotropies in tumour growth	e.g. anisotropic diffusion tensor is used based on brain structure.	by allowing for feedback between the cells and environment, one can introduce preferential migration, leading to anisotropic growth along structures.
cell hierarchy and lineage	a set of coupled PDEs described sub-populations with different properties.	individual cells underlie rules that are affected by cell type.
mitosis and apoptosis	e.g. logarithmic or exponential source terms are included in the PDE. These might link different sub-populations and be associated with properties of the environment.	both phenomena underlie stochastic or deterministic rules that are invoked for each agent.

A key concern in clinical practice is the prediction of tumour growth patterns, sites of progression and the location of tumour recurrence. This triad is important for both therapeutic planning and prognostication [219]. Mathematical models have the potential to refine these facets of care and hence to offer highly tailored conformal radiation dosing and targeted surgical supra-marginal resection [220,221]. These therapeutic adaptations might maximize the prognostic benefits and lead to the destruction of the tumour while sparing normal neural tissue. Similarly, when combined with the modelling of growth rates, this information could be assimilated to generate more accurate prognostic maps with the prediction of anatomico-pathological functional deficits and overall prognosis.

Recent years have been characterized by increasing recognition of GBM's molecular intra- and inter-tumoural heterogeneity and its functional consequences. This is exemplified in the evolution of the WHO classification of tumours from a purely histopathological to a fully integrated molecular classification [222]. As we have summarized, mathematical models of GBM hold the potential to illustrate novel prognostic aspects of tumour biology and the microenvironment not currently captured. These might include structural metrics, such as tissue density and cellular lineage, or functional ones, including oxygenation, nutrient supply and metabolism.

The potential for applying spatio-temporal mathematical modelling of GBM in clinical care is substantial but thus far remains largely unrealized. As summarized in this review, the foundation of knowledge in this area is now considerable. The stage is set for those who wish to advance the field from theoretical models to practical applications.

## 7. Summary and discussion

This article presents an overview of mathematical models that provide means to scrutinize and predict the spatial and temporal evolution of tumours. While we focus on models for GBM and highlight characteristics of this aggressive cancer type, we also attempt to give a rounded picture of state-of-the-art approaches across the field of mathematical oncology.

Spatially resolved tumour models fall into two main categories: they either treat the tumour cell density as a continuous variable (cf. §2), or deal with autonomous agents representing individual cells or cell clusters (cf. §3).

The computational cost associated with continuous models is relatively low. This property allows for the modelling of the entire tumour volume and the application to a wide variety of (patient-specific) data. Furthermore, continuous models can capture many of the characteristics of GBM. We summarize how continuous models achieve this goal in table 3. GBM spreads anisotropically following existing structures in the brain, including white matter tracks and blood vessels. On a macroscopic level, this behaviour is well described by reaction–diffusion equations when including an anisotropic diffusion term (cf. §2.1).

Moreover, by including source terms that couple a set of such reaction–diffusion equations, continuous models can link different cell sub-populations and account for interactions with the environment (cf. §2.3). Continuous models are hereby able to encapsulate the hierarchical nature that is a defining feature of GBM (cf. §2.2). The models also show great versatility: by including additional biologically motivated terms into the reaction–diffusion equations, continuous models can be painlessly extended to include phenomena ranging from immune responses to the impact of radiotherapy.

Tumour cells must always be understood in relation to their surroundings. In this connection, aspects such as nutrition flows, the ECM or the vasculature are often (if not always) represented using continuous models. Even when using agent-based models, continuous models thus play a vital role. However, continuous models have their drawbacks. They do not account for the stochastic events that dominate at low tumour cell densities. Consequently, they are not ideal for addressing some questions regarding the invasive tumour front or tumour recurrence that is a prevalent obstacle in treating GBM.

At low cell densities, agent-based models have an edge. Such models come in many different flavours. Some agent-based models borrow from the description of other phenomena. They thus lean on theoretical models, e.g. from solid-state physics, posing biological events in terms of physical forces and potentials (cf. §§3.1.3, 3.2.1 and 3.2.2). Other models rely on purely stochastic rules to encode biological information (cf. §§3.1.1 and 3.1.2). Moreover, agent-based models differ in the details that they encompass. While some models address aspects of cell morphology, others do not. While some models define a lower threshold for their spatial resolution by employing a lattice on which the agents move, others do not.

Like continuous models, agent-based models are able to capture the essential properties of GBM (table 3). Anisotropic diffusion along existing structures can be included by altering the rules that govern cell migration based on the environment. Moreover, by altering these rules based on the cell type, the hierarchical organization of GBM can be incorporated into the model.

The high computational expense of agent-based models constitutes their main drawback. It can be a significant stumbling block on the way to unleashing their full potential. However, this shortcoming can be partly circumvented. One might thus combine different approaches into a hybrid model bridging across the scales involved (cf. §§4.1 and 4.2). Alternatively, one might study small cell populations to derive emergent macroscopic properties that can be used to calibrate models on a coarser scale (cf. §4.3). Indeed, one of the main assets of agent-based models is their ability to link an understanding of individual cells to macroscopic events. To further lower the computational cost when confronting the models with data, one might use sophisticated statistical techniques or machine-learning methods that demonstrably reduce the number of models that need to be constructed [198,223], as discussed in §5.

Each of the available mathematical models has its strengths and weaknesses. Which model to employ will hence be dictated by the research question and the available data. Firstly, some approaches are better suited for depicting certain phenomena than other methods are. One might drastically simplify the work associated with the practical implementation by choosing the method wisely. Secondly, not all models are equally informative. The question is whether the additional information can be exploited and for what purpose [224]. On the one hand, the chosen model sets limits on the insights that one might gain. This notion favours more complex models. On the other hand, one should avoid cracking nuts with a sledgehammer. To exemplify this, it is thus worth noting that *non-spatial models* make full use of certain types of (patient-specific) data while being unable to address any questions on tumour morphology. They are undoubtedly very valuable tools in their own right. The same holds for each spatio-temporal cancer model presented earlier. With this in mind, we hope that our review provides a useful guide and helps the reader select a suitable mathematical model for their research.

This article aims to give an extensive overview of state-of-the-art modelling techniques. However, we left out some ideas and concepts that go beyond the scope of this review. For instance, one could use agent-based models incorporating evolutionary dynamics [225] or even evolutionary game theory [226].

Mathematical models are only useful if they describe and relate to experimental data. Our review thus ends with a summary and discussion of the application of mathematical models to experimental data and its clinical relevance. A wealth of imaging and molecular data is becoming available, particularly due to advances in single-cell and spatial transcriptomics. At the same time, researchers have begun to implement spatial models into statistical frameworks to perform systematic inference based on these data. While few such inference analyses have yet been published, advances in machine learning and computing power promise to further enable the systematic incorporation of imaging and molecular data into the spatial models of GBM. We thus envision a greater impact of mathematical modelling in unravelling the basic biology of GBM and its applications in clinical treatment in the near future.

**Data accessibility.** This article has no additional data.

**Authors' contributions.** A.C.S.J.: conceptualization, investigation, project administration, visualization, writing—original draft and writing—review and editing; C.S.H.: investigation, project administration and writing—review and editing; M.S.: investigation, project administration and writing—review and editing; W.T.: investigation and writing—review and editing; S.R.K.: writing—review and editing; D.G.: writing—review and editing; M.F.L.: funding acquisition, project administration and writing—review and editing; S.P.: funding acquisition, project administration and writing—review and editing; S.M.: funding acquisition, project administration and writing—review and editing; V.S.: conceptualization, investigation, project administration, supervision and writing—review and editing.

All authors gave final approval for publication and agreed to be held accountable for the work performed therein.

**Conflict of interest declaration.** We declare we have no competing interests.

**Funding.** This work was supported by The Oli Hilsdon Foundation through The Brain Tumour Charity (grant no. GN-000595), in connection with the program 'Mapping the Spatio-temporal Heterogeneity of Glioblastoma Invasion'. Work at the Cancer Institute Genomics Translational Technology Platform was supported by the Cancer Research UK (CRUK) City of London Centre Award (C7893/A26233). C.S.H. was supported by a CRUK Pioneer Award (C70568/A29787), an AMS Starter Grant (SGL021\1034), a National Brain Appeal Innovation Award (NBA/NSG/BTB) and UCLH BRC NIHR funding. S.R.K. was supported by The Edinburgh-UCL CRUK Brain Tumour Centre of Excellence award (C7893/A27590). M.F.L. was supported by the Rosetrees Trust and the John Black Charitable Foundation (grant no. A2200). S.P. was supported by CRUK (awards C55501/A21203 and 7550844).

## References

- Davis M. 2016 Glioblastoma: overview of disease and treatment. *Clin. J. Oncol. Nurs.* **20**, S2–S8. (doi:10.1188/16.CJON.S1.2-8)
- Lan X *et al.* 2017 Fate mapping of human glioblastoma reveals an invariant stem cell hierarchy. *Nature* **549**, 227–232. (doi:10.1038/nature23666)
- Wang M, Dignam J, Won M, Curran W, Mehta M, Gilbert M. 2015 Variation over time and interdependence between disease progression and death among patients with glioblastoma on RT0G 0525. *Neuro Oncol.* **17**, 999–1006. (doi:10.1093/neuonc/nov009)
- Stupp R *et al.* 2005 Radiotherapy plus concomitant and adjuvant temozolomide for glioblastoma. *N Engl. J. Med.* **352**, 987–996. (doi:10.1056/NEJMoa043330)
- Stupp R *et al.* 2009 Effects of radiotherapy with concomitant and adjuvant temozolomide versus radiotherapy alone on survival in glioblastoma in a randomised phase III study: 5-year analysis of the EORTC-NCIC trial. *Lancet Oncol.* **10**, 459–466. (doi:10.1016/S1470-2045(09)70025-7)
- Anderson ARA, Quaranta V. 2008 Integrative mathematical oncology. *Nat. Rev. Cancer* **8**, 227–234. (doi:10.1038/nrc2329)
- Altrock PM, Liu LL, Michor F. 2015 The mathematics of cancer: integrating quantitative models. *Nat. Rev. Cancer* **15**, 730–745. (doi:10.1038/nrc4029)
- Anderson ARA, Maini PK. 2018 Mathematical oncology. *Bull. Math. Biol.* **80**, 945–953. (doi:10.1007/s11538-018-0423-5)
- Cranmer K, Brehmer J, Louppe G. 2020 The frontier of simulation-based inference. *Proc. Natl Acad. Sci. USA* **117**, 30 055–30 062. (doi:10.1073/pnas.1912789117)
- Zadeh Shirazi A, Fornaciari E, McDonnell MD, Yaghoobi M, Cevallos Y, Tello-Quendo L, Inca D, Gomez GA. 2020 The application of deep convolutional neural networks to brain cancer images: a survey. *J. Per. Med.* **10**, 224. (doi:10.3390/jpm10040224)
- Finch A, Solomou G, Wykes V, Pohl U, Bardella C, Watts C. 2021 Advances in research of adult gliomas. *Int. J. Mol. Sci.* **22**, E924. (doi:10.3390/ijms22020924)
- Metzcar J, Wang Y, Heiland R, Macklin P. 2019 A review of cell-based computational modeling in cancer biology. *JCO Clin. Cancer Inf.* **3**, 1–13.
- Weerasinghe WMH, Burrage P, Burrage K, Nicolau D. 2019 Mathematical models of cancer cell plasticity. *J. Oncol.* **2019**, 1–14. (doi:10.1155/2019/2403483)
- Falco J *et al.* 2021 *In silico* mathematical modelling for glioblastoma: a critical review and a patient-specific case. *J. Clin. Med.* **10**, 2169. (doi:10.3390/jcm10102169)
- Jarrett AM, Lima EA, Hormuth DA, McKenna MT, Feng X, Ekrut DA, Resende AC, Brock A, Yankeelov TE. 2018 Mathematical models of tumor cell proliferation: a review of the literature. *Expert Rev. Anticancer Ther.* **18**, 1271–1286. (doi:10.1080/14737140.2018.1527689)
- Karolak A, Markov DA, McCawley LJ, Rejniak KA. 2018 Towards personalized computational oncology: from spatial models of tumour spheroids, to organoids, to tissues. *J. R. Soc. Interface* **15**, 20170703. (doi:10.1098/rsif.2017.0703)
- Lowengrub JS, Frieboes HB, Jin F, Chuang YL, Li X, Macklin P, Wise SM, Cristini V. 2010 Nonlinear modelling of cancer: bridging the gap between cells and tumours. *Nonlinearity* **23**, R1–R9. (doi:10.1088/0951-7715/23/1/R01)
- Liedekerke P, Palm M, Jagiella N, Drasdo D. 2015 Simulating tissue mechanics with agent-based models: concepts, perspectives and some novel results. *Comput. Particle Mech.* **2**, 401–444.
- Deisboeck T, Wang Z, Macklin P, Cristini V. 2010 Multiscale cancer modeling. *Annu. Rev. Biomed. Eng.* **13**, 127–55. (doi:10.1146/annurev-bioeng-071910-124729)
- Chamseddine I, Rejniak K. 2019 Hybrid modeling frameworks of tumor development and treatment. *Wiley Interdiscip. Rev.: Syst. Biol. Med.* **12**, e1461.
- Falco J *et al.* 2021 *In silico* mathematical modelling for glioblastoma: a critical review and a patient-specific case. *J. Clin. Med.* **10**, 2169. (doi:10.3390/jcm10102169)
- Ellis H, Greenslade M, Powell B, Spiteri I, Sottoriva A, Kurian K. 2015 Current challenges in glioblastoma: intratumour heterogeneity, residual disease, and models to predict disease recurrence. *Front. Oncol.* **5**, 251. (doi:10.3389/fonc.2015.00251)
- Alfonso JC, Talkenberger K, Seifert M, Klink B, Hawkins-Daarud A, Swanson KR, Hatzikirou H, Deutsch A. 2017 The biology and mathematical modelling of glioma invasion: a review. *J. R. Soc. Interface* **14**, 20170490. (doi:10.1098/rsif.2017.0490)
- McKinnon C, Nandhabalan M, Murray SA, Plaha P. 2021 Glioblastoma: clinical presentation, diagnosis, and management. *BMJ (Clinical research ed)* **374**, n1560. (doi:10.1136/bmj.n1560)
- Frieboes HB, Lowengrub JS, Wise S, Zheng X, Macklin P, Bearer EL, Cristini V. 2007 Computer simulation of glioma growth and morphology. *NeuroImage* **37**(Suppl 1), S59–S70. (doi:10.1016/j.neuroimage.2007.03.008)
- Swan A, Hillen T, Bowman JC, Murtha AD. 2018 A patient-specific anisotropic diffusion model for brain tumour spread. *Bull. Math. Biol.* **80**, 1259–1291. (doi:10.1007/s11538-017-0271-8)
- Swanson K, Alvord E, Murray J. 2002 Virtual brain tumours (gliomas) enhance the reality of medical imaging and highlight inadequacies of current therapy. *Br. J. Cancer* **86**, 14–18. (doi:10.1038/sj.bjc.6600021)
- Frieboes HB, Zheng X, Sun CH, Tromberg B, Gatenby R, Cristini V. 2006 An integrated computational/experimental model of tumor invasion. *Cancer Res.* **66**, 1597–1604. (doi:10.1158/0008-5472.CAN-05-3166)
- Swanson K, Alvord E, Murray J. 2000 A quantitative model for differential motility of gliomas in grey and white matter. *Cell Prolif.* **33**, 317–329. (doi:10.1046/j.1365-2184.2000.00177.x)

30. Gu S *et al.* 2012 Applying a patient-specific bio-mathematical model of glioma growth to develop virtual [18F]-FMISO-PET images. *Math. Med. Biol.: A J. IMA* **29**, 31–48. (doi:10.1093/imammb/dqr002)
31. Corwin D, Holdsworth C, Rockne RC, Trister AD, Mrugala MM, Rockhill JK, Stewart RD, Phillips M, Swanson KR. 2013 Toward patient-specific, biologically optimized radiation therapy plans for the treatment of glioblastoma. *PLoS ONE* **8**, e79115. (doi:10.1371/journal.pone.0079115)
32. Neal ML *et al.* 2013 Discriminating survival outcomes in patients with glioblastoma using a simulation-based, patient-specific response metric. *PLoS ONE* **8**, e51951. (doi:10.1371/journal.pone.0051951)
33. Jackson PR, Juliano J, Hawkins-Daarud A, Rockne RC, Swanson KR. 2015 Patient-specific mathematical neuro-oncology: using a simple proliferation and invasion tumor model to inform clinical practice. *Bull. Math. Biol.* **77**, 846–856. (doi:10.1007/s11538-015-0067-7)
34. Wang Z, Deisboeck TS. 2009 *Computational modeling of brain tumors: discrete, continuum or hybrid?*, pp. 381–393. Netherlands: Springer.
35. Zheng X, Wise S, Cristini V. 2005 Nonlinear simulation of tumor necrosis, neo-vascularization and tissue invasion via an adaptive finite-element/level-set method. *Bull. Math. Biol.* **67**, 211–259. (doi:10.1016/j.bulm.2004.08.001)
36. Dattoli G, Licciardi S, Guiot C, Deisboeck TS. 2014 Capillary network, cancer and kleiber law. (<http://arxiv.org/abs/1403.4443>).
37. Powathil G, Kohandel M, Milosevic M, Sivaloganathan S. 2012 Modeling the spatial distribution of chronic tumor hypoxia: implications for experimental and clinical studies. *Comput. Math. Methods Med.* **2012**, 410602. (doi:10.1155/2012/410602)
38. Gerlee P, Nelander S. 2012 The impact of phenotypic switching on glioblastoma growth and invasion. *PLoS Comput. Biol.* **8**, e1002556. (doi:10.1371/journal.pcbi.1002556)
39. Cristini V, Lowengrub J, Nie Q. 2003 Nonlinear simulation of tumor growth. *J. Math. Biol.* **46**, 191–224. (doi:10.1007/s00285-002-0174-6)
40. Sinek J, Frieboes H, Zheng X, Cristini V. 2004 Two-dimensional chemotherapy simulations demonstrate fundamental transport and tumor response limitations involving nanoparticles. *Biomed. Microdevices* **6**, 297–309. (doi:10.1023/B:BMMD.0000048562.29657.64)
41. Cristini V, Frieboes HB, Gatenby R, Caserta S, Ferrari M, Sinek J. 2005 Morphologic instability and cancer invasion. *Clin. Cancer Res.* **11**(19 Pt 1), 6772–6779. (doi:10.1158/1078-0432.CCR-05-0852)
42. Mahlbacher G, Curtis LT, Lowengrub J, Frieboes HB. 2018 Mathematical modeling of tumor-associated macrophage interactions with the cancer microenvironment. *J. Immunother. Cancer* **6**, 10. (doi:10.1186/s40425-017-0313-7)
43. Bull JA, Mech F, Quaiser T, Waters S, Byrne H. 2020 Mathematical modelling reveals cellular dynamics within tumour spheroids. *PLoS Comput. Biol.* **16**, e1007961. (doi:10.1371/journal.pcbi.1007961)
44. Suarez C, Maglietti F, Colonna M, Breitbart K, Marshall G. 2012 Mathematical modeling of human glioma growth based on brain topological structures: study of two clinical cases. *PLoS ONE* **7**, e39616. (doi:10.1371/journal.pone.0039616)
45. Rutter E *et al.* 2017 Mathematical analysis of glioma growth in a murine model. *Sci. Rep.* **7**, 1–6. (doi:10.1038/s41598-017-02462-0)
46. Giatili S, Stamatakos G. 2012 A detailed numerical treatment of the boundary conditions imposed by the skull on a diffusion–reaction model of glioma tumor growth. *Clinical validation aspects. Appl. Math. Comput.* **218**, 8779–8799.
47. Painter K, Hillen T. 2013 Mathematical modelling of glioma growth: the use of diffusion tensor imaging (DTI) data to predict the anisotropic pathways of cancer invasion. *J. Theor. Biol.* **323**, 25–39. (doi:10.1016/j.jtbi.2013.01.014)
48. Eftimie R, Bramson J, Earn D. 2010 Interactions between the immune system and cancer: a brief review of non-spatial mathematical models. *Bull. Math. Biol.* **73**, 2–32. (doi:10.1007/s11538-010-9526-3)
49. Murphy H, Jaafari H, Dobrovolsky HM. 2016 Differences in predictions of ODE models of tumor growth: a cautionary example. *BMC Cancer* **16**, 163. (doi:10.1186/s12885-016-2164-x)
50. Barros LRC, Paixão EA, Valli AMP, Naozuka GT, Fassoni AC, Almeida RC. 2021 CART-T math-a mathematical model of CAR-T immunotherapy in preclinical studies of hematological cancers. *Cancers* **13**, 2941. (doi:10.3390/cancers13122941)
51. Yu VY, Nguyen D, O'Connor D, Ruan D, Kaprealian T, Chin R, Sheng K. 2021 Treating glioblastoma multiforme (GBM) with super hyperfractionated radiation therapy: implication of temporal dose fractionation optimization including cancer stem cell dynamics. *PLoS ONE* **16**, e0245676. (doi:10.1371/journal.pone.0245676)
52. Sachs R, Hlatky L, Hahnfeldt P. 2001 Simple ODE models of tumor growth and anti-angiogenic or radiation treatment. *Math. Comput. Modell.* **33**, 1297–1305. (doi:10.1016/S0895-7177(00)00316-2)
53. Simeoni M, Magni P, Cammia C, De Nicolao G, Croci V, Pesenti E, Germani M, Poggese I, Rocchetti M. 2004 Predictive pharmacokinetic-pharmacodynamic modeling of tumor growth kinetics in xenograft models after administration of anticancer agents. *Cancer Res.* **64**, 1094–101. (doi:10.1158/0008-5472.CAN-03-2524)
54. Koziol J, Falls T, Schnitzer J. 2020 Different ODE models of tumor growth can deliver similar results. *BMC Cancer* **20**, 226. (doi:10.1186/s12885-020-6703-0)
55. Scherer HJ. 1938 Structural development in gliomas. *Am. J. Cancer* **34**, 333–351.
56. Giese A, Westphal M. 1996 Glioma invasion in the central nervous system. *Neurosurgery* **39**, 235–250. (doi:discussion 250–2)
57. Rao JS. 2003 Molecular mechanisms of glioma invasiveness: the role of proteases. *Nat. Rev. Cancer* **3**, 489–501. (doi:10.1038/nrc1121)
58. Konukoglu E, Clatz O, Bondiau PY, Delingette H, Ayache N. 2010 Extrapolating glioma invasion margin in brain magnetic resonance images: suggesting new irradiation margins. *Med. Image Anal.* **14**, 111–125. (doi:10.1016/j.media.2009.11.005)
59. Gritsenko PG, Ilna O, Friedl P. 2012 Interstitial guidance of cancer invasion. *J. Pathol.* **226**, 185–199. (doi:10.1002/path.3031)
60. Cuddapah VA, Robel S, Watkins S, Sontheimer H. 2014 A neurocentric perspective on glioma invasion. *Nat. Rev. Neurosci.* **15**, 455–465. (doi:10.1038/nrn3765)
61. Brooks LJ *et al.* 2020 The white matter is a pro-differentiative microenvironment for glioblastoma. *bioRxiv*. Available from: <https://www.biorxiv.org/content/early/2020/11/16/2020.11.14.379594>.
62. Tracqui P, Cruywagen G, Woodward D, Bartoo G, Murray J, Alvord E. 1995 A mathematical model of glioma growth: the effect of chemotherapy on spatio-temporal growth. *Cell Prolif.* **28**, 17–31. (doi:10.1111/j.1365-2184.1995.tb00036.x)
63. Jbabdi S, Mandonnet E, Duffau H, Capelle L, Swanson KR, Pelégrini-Issac M, Guillemin R, Benali H. 2005 Simulation of anisotropic growth of low-grade gliomas using diffusion tensor imaging. *Magn. Reson. Med.* **54**, 616–624. (doi:10.1002/mrm.20625)
64. Hogeia C, Davatzikos C, Biros G. 2008 An image-driven parameter estimation problem for a reaction–diffusion glioma growth model with mass effects. *J. Math. Biol.* **56**, 793–825. (doi:10.1007/s00285-007-0139-x)
65. Antonopoulos M, Dionysiou D, Stamatakos G, Uzunoglu N. 2019 Three-dimensional tumor growth in time-varying chemical fields: a modeling framework and theoretical study. *BMC Bioinf.* **20**, 442. (doi:10.1186/s12859-019-2997-9)
66. Beppu T, Inoue T, Shibata Y, Kurose A, Arai H, Ogasawara K, Ogawa A, Nakamura S, Kabasawa H. 2003 Measurement of fractional anisotropy using diffusion tensor MRI in supratentorial astrocytic tumors. *J. Neurooncol.* **63**, 109–116. (doi:10.1023/a:1023977520909)
67. Hillen T, Painter KJ. 2013 *Transport and anisotropic diffusion models for movement in oriented habitats*, pp. 177–222. Berlin, Heidelberg: Springer. (doi:10.1007/978-3-642-35497-7\_7)
68. Engwer C, Hillen T, Knappitsch M, Surulescu C. 2015 Glioma follow white matter tracts: a multiscale DTI-based model. *J. Math. Biol.* **71**, 551–582. (doi:10.1007/s00285-014-0822-7)
69. Engwer C, Knappitsch M, Surulescu C. 2016 A multiscale model for glioma spread including cell-tissue interactions and proliferation. *Math. Biosci. Eng.: MBE* **13**, 443–460. (doi:10.3934/mbe.2015011)
70. Belmonte-Betitia J, Woolley T, Scott J, Maini P, Gaffney E. 2013 Modelling biological invasions: individual to population scales at interfaces. *J. Theor. Biol.* **334**, 1–12. (doi:10.1016/j.jtbi.2013.05.033)
71. Lee M, Chen GT, Puttock E, Wang K, Edwards RA, Waterman ML, Lowengrub J. 2017 Mathematical modeling links Wnt signaling to emergent patterns of metabolism in colon cancer. *Mol. Syst. Biol.* **13**, 912. (doi:10.15252/msb.20167386)
72. Singh SK, Hawkins C, Clarke ID, Squire JA, Bayani J, Hide T, Henkelman RM, Cusimano MD, Dirks PB. 2004 Identification of human brain tumour initiating cells. *Nature* **432**, 396–401. (doi:10.1038/nature03128)

73. Venere M, Fine HA, Dirks PB, Rich JN. 2011 Cancer stem cells in gliomas: identifying and understanding the apex cell in cancer's hierarchy. *Glia* **59**, 1148–1154. (doi:10.1002/glia.21185)
74. Wise S, Lowengrub J, Frieboes H, Cristini V. 2008 Three-dimensional multispecies nonlinear tumor growth—I model and numerical method. *J. Theor. Biol.* **253**, 524–543. (doi:10.1016/j.jtbi.2008.03.027)
75. Wise S, Lowengrub J, Cristini V. 2011 An adaptive multigrid algorithm for simulating solid tumor growth using mixture models. *Math. Comput. Modell.* **53**, 1–20. (doi:10.1016/j.mcm.2010.07.007)
76. Byrne HM, Chaplain M. 1996 Growth of necrotic tumors in the presence and absence of inhibitors. *Math. Biosci.* **135**, 187–216. (doi:10.1016/0025-5564(96)00023-5)
77. Frieboes HB, Smith BR, Chuang YL, Ito K, Roettgers AM, Gambhir SS, Cristini V. 2013 An integrated computational/experimental model of lymphoma growth. *PLoS Comput. Biol.* **9**, e1003008. (doi:10.1371/journal.pcbi.1003008)
78. Kim J, Kang K, Lowengrub J. 2004 Conservative multigrid methods for ternary Cahn-Hilliard systems. *Commun. Math. Sci. - COMMUN. MATH. SCI.* **2**, 53–77.
79. Wise S, Lowengrub J, Kim J, Johnson W. 2004 Efficient phase-field simulation of quantum dot formation in a strained heteroepitaxial film. *Superlattices Microstruct.* **36**, 293–304. (doi:10.1016/j.spmi.2004.08.029)
80. Kim J, Lowengrub J. 2005 Phase field modeling and simulation of three-phase flows. *Interfaces Free Boundaries* **7**, 435–466. (doi:10.4171/IFB/132)
81. Kunche S, Yan H, Calof AL, Lowengrub JS, Lander AD. 2016 Feedback, lineages and self-organizing morphogenesis. *PLoS Comput. Biol.* **12**, e1004814. (doi:10.1371/journal.pcbi.1004814)
82. Yan H, Romero-Lopez M, Frieboes HB, Hughes CW, Lowengrub JS. 2017 Multiscale modeling of glioblastoma suggests that the partial disruption of vessel/cancer stem cell crosstalk can promote tumor regression without increasing invasiveness. *IEEE Trans. Biomed. Eng.* **64**, 538–548.
83. Yan H, Romero-López M, Benitez LI, Di K, Frieboes HB, Hughes CC, Bota DA, Lowengrub JS. 2017 3D mathematical modeling of glioblastoma suggests that transdifferentiated vascular endothelial cells mediate resistance to current standard-of-care therapy. *Cancer Res.* **77**, 4171–4184. (doi:10.1158/0008-5472.CAN-16-3094)
84. Yan H, Konstorum A, Lowengrub JS. 2018 Three-dimensional spatiotemporal modeling of colon cancer organoids reveals that multimodal control of stem cell self-renewal is a critical determinant of size and shape in early stages of tumor growth. *Bull. Math. Biol.* **80**, 1404–1433. (doi:10.1007/s11538-017-0294-1)
85. Chen Y, Wise SM, Shenoy VB, Lowengrub JS. 2014 A stable scheme for a nonlinear, multiphase tumor growth model with an elastic membrane. *Int. J. Numer. Methods Biomed. Eng.* **30**, 726–754. (doi:10.1002/cnm.2624)
86. Chen Y, Lowengrub JS. 2014 Tumor growth in complex, evolving microenvironmental geometries: a diffuse domain approach. *J. Theor. Biol.* **361**, 14–30. (doi:10.1016/j.jtbi.2014.06.024)
87. Chen Y, Lowengrub JS. 2019 Tumor growth and calcification in evolving microenvironmental geometries. *J. Theor. Biol.* **463**, 138–154. (doi:10.1016/j.jtbi.2018.12.006)
88. Ravi VM *et al.* 2021 Spatiotemporal heterogeneity of glioblastoma is dictated by microenvironmental interference. bioRxiv. <https://www.biorxiv.org/content/early/2021/02/17/2021.02.16.431475>.
89. Anderson ARA, Weaver AM, Cummings PT, Quaranta V. 2006 Tumor morphology and phenotypic evolution driven by selective pressure from the microenvironment. *Cell* **127**, 905–915. (doi:10.1016/j.cell.2006.09.042)
90. Jiang Y, Pjesivac-Grbovic J, Cantrell C, Freyer J. 2006 A multiscale model for avascular tumor growth. *Biophys. J.* **89**, 3884–3894. (doi:10.1529/biophysj.105.060640)
91. Powathil GG, Gordon KE, Hill LA, Chaplain MA. 2012 Modelling the effects of cell-cycle heterogeneity on the response of a solid tumour to chemotherapy: biological insights from a hybrid multiscale cellular automaton model. *J. Theor. Biol.* **308**, 1–19. (doi:10.1016/j.jtbi.2012.05.015)
92. Mantzaris N, Webb S, Othmer H. 2004 Mathematical modeling of tumor-induced angiogenesis. *J. Math. Biol.* **49**, 111–87. (doi:10.1007/s00285-003-0262-2)
93. Chaplain MAJ. 1996 Avascular growth, angiogenesis and vascular growth in solid tumours: the mathematical modelling of the stages of tumour development. *Math. Comput. Modell.* **23**, 47–87. (doi:10.1016/0895-7177(96)00019-2)
94. Orme M, Chaplain M. 1997 Two-dimensional models of tumour angiogenesis and anti-angiogenesis strategies. *IMA J. Math. Appl. Med. Biol.* **14**, 189–205. (doi:10.1093/imammb/14.3.189)
95. Scianna M, Bell CG, Preziosi L. 2013 A review of mathematical models for the formation of vascular networks. *J. Theor. Biol.* **333**, 174–209. (doi:10.1016/j.jtbi.2013.04.037)
96. Flegg JA, Menon SN, Byrne HM, McElwain DLS. 2020 A current perspective on wound healing and tumour-induced angiogenesis. *Bull. Math. Biol.* **82**, 23. (doi:10.1007/s11538-020-00696-0)
97. Shirinifard A, Gens J, Zaitlen B, Poplawski N, Swat M, Glazier J. 2009 3D multi-cell simulation of tumor growth and angiogenesis. *PLoS ONE* **4**, e7190. (doi:10.1371/journal.pone.0007190)
98. Daub J, Merks R. 2013 A cell-based model of extracellular-matrix-guided endothelial cell migration during angiogenesis. *Bull. Math. Biol.* **75**, 1377–1399. (doi:10.1007/s11538-013-9826-5)
99. Xu J, Vilanova G, Gomez H. 2016 A mathematical model coupling tumor growth and angiogenesis. *PLoS ONE* **11**, 1–20. (doi:10.1371/journal.pone.0149422)
100. Pillay S, Byrne HM, Maini PK. 2017 Modeling angiogenesis: a discrete to continuum description. *Phys. Rev. E* **95**, 012410. (doi:10.1103/PhysRevE.95.012410)
101. Chamseddine IM, Frieboes HB, Kokkolaras M. 2018 Design optimization of tumor vasculature-bound nanoparticles. *Sci. Rep.* **8**, 17768. (doi:10.1038/s41598-018-35675-y)
102. Anderson A, Chaplain M. 1998 Continuous and discrete mathematical models of tumor-induced angiogenesis. *Bull. Math. Biol.* **60**, 857–899. (doi:10.1006/bulm.1998.0042)
103. Trucu D, Lin P, Chaplain M, Wang Y. 2013 A multiscale moving boundary model arising in cancer invasion. *Multiscale Model. Simul.* **11**, 309–35. (doi:10.1137/110839011)
104. Hanahan D, Weinberg R. 2011 Hallmarks of cancer: the next generation. *Cell* **144**, 646–74. (doi:10.1016/j.cell.2011.02.013)
105. Macklin P, Frieboes HB, Sparks JL, Ghaffarizadeh A, Friedman SH, Juarez EF, Jonckheere E, Mumenthaler SM. 2016 *Progress towards computational 3-D multicellular systems biology*, vol. 936, pp. 225–246. United States of America: Springer.
106. Kansal A, Torquato S, Harsh IV G, Chiocca E, Deisboeck T. 2000 Cellular automaton of idealized brain tumor growth dynamics. *Bio. Systems* **55**, 119–127. (doi:10.1016/s0303-2647(99)00089-1)
107. Kansal A, Torquato S, Harsh GR I, Chiocca E, Deisboeck T. 2000 Simulated brain tumor growth dynamics using a three-dimensional cellular automaton. *J. Theor. Biol.* **203**, 367–382. (doi:10.1006/jtbi.2000.2000)
108. Mansury Y, Kimura M, Lobo J, Deisboeck TS. 2002 Emerging patterns in tumor systems: simulating the dynamics of multicellular clusters with an agent-based spatial agglomeration model. *J. Theor. Biol.* **219**, 343–370. (doi:10.1006/jtbi.2002.3131)
109. Schmitz JE, Kansal AR, Torquato S. 2002 A cellular automaton model of brain tumor treatment and resistance. *J. Theor. Med.* **4**, 223–239. (doi:10.1080/1027366031000086674)
110. Hatzikirou H, Deutsch A. 2010 *Lattice-gas cellular automaton modeling of emergent behavior in interacting cell populations*, vol. 2010, pp. 301–331. Germany: Springer.
111. Hatzikirou H, Basanta D, Simon M, Schaller K, Deutsch A. 2012 'Go or Grow': the key to the emergence of invasion in tumour progression? *Math. Med. Biol.: A J. IMA* **29**, 49–65. (doi:10.1093/imammb/dqg011)
112. Jagiella N, Müller B, Müller M, Vignon-Clementel IE, Drasdo D. 2016 Inferring growth control mechanisms in growing multi-cellular spheroids of NSCLC cells from spatial-temporal image data. *PLoS Comput. Biol.* **12**, e1004412. (doi:10.1371/journal.pcbi.1004412)
113. Pillay S, Byrne HM, Maini PK. 2018 The impact of exclusion processes on angiogenesis models. *J. Math. Biol.* **77**, 1721–1759. (doi:10.1007/s00285-018-1214-1)
114. Macklin P, Edgerton ME, Thompson AM, Cristini V. 2012 Patient-calibrated agent-based modelling of ductal carcinoma in situ (DCIS): from microscopic measurements to macroscopic predictions of clinical progression. *J. Theor. Biol.* **301**, 122–140. (doi:10.1016/j.jtbi.2012.02.002)
115. Hyun AZ, Macklin P. 2013 Improved patient-specific calibration for agent-based cancer

- modeling. *J. Theor. Biol.* **317**, 422–424. (doi:10.1016/j.jtbi.2012.10.017)
116. Cooper FR *et al.* 2020 Chaste: cancer, heart and soft tissue environment. *J. Open Sourc. Softw.* **5**, 1848. (doi:10.21105/joss.01848)
117. Ghaffarizadeh A, Heiland R, Friedman SH, Mumenthaler SM, Macklin P. 2018 PhysCell: an open source physics-based cell simulator for 3-D multicellular systems. *PLoS Comput. Biol.* **14**, e1005991. (doi:10.1371/journal.pcbi.1005991)
118. Graner F, Glazier JA. 1992 Simulation of biological cell sorting using a two-dimensional extended Potts model. *Phys. Rev. Lett.* **69**, 2013–2016. (doi:10.1103/PhysRevLett.69.2013)
119. Ghaffarizadeh A, Heiland R, Friedman S, Mumenthaler S, Macklin P. 2018 PhysCell: an open source physics-based cell simulator for 3-D multicellular systems. *PLoS Comput. Biol.* **14**, e1005991. (doi:10.1371/journal.pcbi.1005991)
120. Block M, Schöll E, Drasdo D. 2008 Classifying the expansion kinetics and critical surface dynamics of growing cell populations. *Phys. Rev. Lett.* **99**, 248101. (doi:10.1103/PhysRevLett.99.248101)
121. Poleszczuk J, Macklin P, Enderling H. 2016 *Agent-based modeling of cancer stem cell driven solid tumor growth*, vol. 1516, pp. 335–346. United States of America: Springer.
122. Drasdo D. 2005 Coarse graining in simulated cell populations. *Adv. Complex Syst. (ACS)* **8**, 319–363. (doi:10.1142/S0219525905000440)
123. Jagiella N, Rickert D, Theis FJ, Hasenauer J. 2017 Parallelization and high-performance computing enables automated statistical inference of multi-scale models. *Cell Syst.* **4**, 194–206.e9. (doi:10.1016/j.cels.2016.12.002)
124. Hoehme S, Drasdo D. 2010 Biomechanical and nutrient controls in the growth of mammalian cell populations. *Math. Popul. Stud.* **17**, 166–187. (doi:10.1080/0898480.2010.491032)
125. Radszweim M, Block M, Hengstler J, Schöll E, Drasdo D. 2009 Comparing the growth kinetics of cell populations in two and three dimensions. *Phys. Rev. E* **79**, 051907. (doi:10.1103/PhysRevE.79.051907)
126. Gillespie DT, Gillespie DT. 1977 Exact stochastic simulation of coupled chemical reactions. *J. Phys. Chem.* **81**, 2340–2361.
127. Bonabeau E. 2002 Agent-based modeling: methods and techniques for simulating human systems. *Proc. Natl Acad. Sci. USA* **99**(Suppl 3), 7280–7287. (doi:10.1073/pnas.082080899)
128. Gibson MA, Bruck J. 2000 Efficient exact stochastic simulation of chemical systems with many species and many channels. *J. Phys. Chem. A* **104**, 1876–1889. (doi:10.1021/jp993732q)
129. Spill F, Guerrero P, Alarcon T, Maini PK, Byrne HM. 2015 Mesoscopic and continuum modelling of angiogenesis. *J. Math. Biol.* **70**, 485–532. (doi:10.1007/s00285-014-0771-1)
130. Dodelson S. 2003 *Modern cosmology*. San Diego, CA: Academic Press.
131. Chopard B, Ouared R, Deutsch A, Hatzikirou H, Wolf-Gladrow D. 2010 Lattice-gas cellular automaton models for biology: from fluids to cells. *Acta Biotheor.* **58**, 329–40. (doi:10.1007/s10441-010-9118-5)
132. Tektonidis M, Hatzikirou H, Chauvière A, Simon M, Schaller K, Deutsch A. 2011 Identification of intrinsic in vitro cellular mechanisms for glioma invasion. *J. Theor. Biol.* **287**, 131–147. (doi:10.1016/j.jtbi.2011.07.012)
133. Giese A, Bjerkvig R, Berens M, Westphal M. 2003 Cost of migration: invasion of malignant gliomas and implications for treatment. *J. Clin. Oncol.* **21**, 1624–36. (doi:10.1200/JCO.2003.05.063)
134. Godlewski J *et al.* 2010 MicroRNA-451 regulates LKB1/AMPK signaling and allows adaptation to metabolic stress in glioma cells. *Mol. Cell* **37**, 620–632. (doi:10.1016/j.molcel.2010.02.018)
135. Monteiro A, Hill R, Pilkington G, Madureira P. 2017 The role of hypoxia in glioblastoma invasion. *Cells* **6**, 45. (doi:10.3390/cells6040045)
136. Taylor JR. 2005 *Classical mechanics*. United States of America: University Science Books.
137. Turner S, Sherratt J. 2002 Intercellular adhesion and cancer invasion: a discrete simulation using the extended Potts model. *J. Theor. Biol.* **216**, 85–100. (doi:10.1006/jtbi.2001.2522)
138. Gao X, McDonald J, Hlatky L, Enderling H. 2012 Acute and fractionated irradiation differentially modulate glioma stem cell division kinetics. *Cancer Res.* **73**, 1481–1490. (doi:10.1158/0008-5472.CAN-12-3429)
139. Gregory P. 2005 *Bayesian logical data analysis for the physical sciences: a comparative approach with mathematica® Support*. Cambridge, UK: Cambridge University Press.
140. Ouchi NB, Glazier J, Rieu J, Upadhyaya A, Sawada Y. 2003 Improving the realism of the cellular Potts model in simulations of biological cells. *Phys. A: Stat. Mech. Appl.* **329**, 451–458. (doi:10.1016/S0378-4371(03)00574-0)
141. Boghaert E, Radisky DC, Nelson CM. 2014 Lattice-based model of ductal carcinoma in situ suggests rules for breast cancer progression to an invasive state. *PLoS Comput. Biol.* **10**, e1003997. (doi:10.1371/journal.pcbi.1003997)
142. Savill NJ, Hogeweg P. 1997 Modelling morphogenesis: from single cells to crawling slugs. *J. Theor. Biol.* **184**, 229–235. (doi:10.1006/jtbi.1996.0237)
143. Szabó A, Merks RMH. 2013 Cellular potts modeling of tumor growth, tumor invasion, and tumor evolution. *Front. Oncol.* **3**, 87.
144. Li JF, Lowengrub J. 2014 The effects of cell compressibility, motility and contact inhibition on the growth of tumor cell clusters using the cellular Potts model. *J. Theor. Biol.* **343**, 79–91. (doi:10.1016/j.jtbi.2013.10.008)
145. Rens EG, Edelstein-Keshet L. 2019 From energy to cellular forces in the cellular potts model: an algorithmic approach. *PLoS Comput. Biol.* **15**, 1–23. (doi:10.1371/journal.pcbi.1007459)
146. Tsingos E, Bakker BH, Keijzer KAE, Hupkes HJ, Merks RMH. 2022 Modelling the mechanical cross-talk between cells and fibrous extracellular matrix using hybrid cellular Potts and molecular dynamics methods. bioRxiv. Available from <https://www.biorxiv.org/content/early/2022/07/07/2022.06.10.495667>.
147. Dallon J, Othmer H. 2004 How cellular movement determines the collective force generated by the Dictyostelium discoideum slug. *J. Theor. Biol.* **231**, 203–22. (doi:10.1016/j.jtbi.2004.06.015)
148. Drasdo D, Hoehme S. 2005 A single-cell-based model of tumor growth in vitro: Monolayers and spheroids. *Phys. Biol.* **2**, 133–47. (doi:10.1088/1478-3975/2/3/001)
149. Mathias S, Coulier A, Bouchnita A, Hellander A. 2020 Impact of force function formulations on the numerical simulation of centre-based models. bioRxiv. Available from <https://www.biorxiv.org/content/early/2020/03/18/2020.03.16.993246>.
150. Meineke F, Potten C, Loeffler M. 2001 Cell migration and organization in the intestinal crypt using a lattice-free model. *Cell Prolif.* **34**, 253–266. (doi:10.1046/j.0960-7722.2001.00216.x)
151. Gallaher JA *et al.* 2020 From cells to tissue: how cell scale heterogeneity impacts glioblastoma growth and treatment response. *PLoS Comput. Biol.* **16**, e1007672. (doi:10.1371/journal.pcbi.1007672)
152. Perez-Velazquez J, Rejniak K. 2020 Drug-induced resistance in micrometastases: analysis of spatio-temporal cell lineages. *Front. Physiol.* **11**, 319.
153. Buenemann M, Lenz P. 2008 Elastic properties and mechanical stability of chiral and filled viral capsids. *Phys. Rev. E, Stat. Nonlin. Soft Matter Phys.* **78**(5 Pt 1), 051924. (doi:10.1103/PhysRevE.78.051924)
154. Van Liedekerke P, Neitsch J, Johann T, Warmt E, González-Valverde I, Hoehme S, Grosser S, Kaes J, Drasdo D. 2020 A quantitative high-resolution computational mechanics cell model for growing and regenerating tissues. *Biomech. Model. Mechanobiol.* **19**, 189–220. (doi:10.1007/s10237-019-01204-7)
155. Liedekerke P, Tijssens E, Ramon H, Ghysels P, Samaey G, Roose D. 2010 Particle-based model to simulate the micromechanics of biological cells. *Phys. Rev. E, Stat. Nonlin. Soft Matter Phys.* **81**, 061906.
156. Odenthal T, Smeets B, Van Liedekerke P, Tijssens E, Van Oosterwyck H, Ramon H. 2013 Analysis of initial cell spreading using mechanistic contact formulations for a deformable cell model. *PLoS Comput. Biol.* **9**, e1003267. (doi:10.1371/journal.pcbi.1003267)
157. Osborne J *et al.* 2010 A hybrid approach to multi-scale modelling of cancer. *Phil. Trans. Ser. A, Math., Phys., Eng. Sci.* **368**, 5013–5028. (doi:10.1098/rsta.2010.0173)
158. Alt S, Ganguly P, Salbreux G. 2017 Vertex models: from cell mechanics to tissue morphogenesis. *Phil. Trans. R. Soc. B* **372**, 20150520. (doi:10.1098/rstb.2015.0520)
159. Osborne JM, Maini PK, Gavaghan DJ. 2017 Comparing individual-based approaches to modelling the self-organization of multicellular tissues. *PLoS Comput. Biol.* **13**, e1005387. (doi:10.1371/journal.pcbi.1005387)
160. Wang Z, Butner JD, Kerketta R, Cristini V, Deisboeck TS. 2015 Simulating cancer growth with multiscale agent-based modeling. *Semin. Cancer Biol.* **30**, 70–78. (doi:10.1016/j.semcancer.2014.04.001)
161. Harris L, Beik S, Murobushi Ozawa PM, Jimenez L, Weaver A. 2019 Modeling heterogeneous tumor growth dynamics and cell-cell interactions at single-cell and cell-population resolution. *Curr. Opin. Syst. Biol.* **17**, 24–34. (doi:10.1016/j.coisb.2019.09.005)

162. Jiao Y, Torquato S. 2013 Evolution and morphology of microenvironment-enhanced malignancy of three-dimensional invasive solid tumors. *Phys. Rev. E, Stat., Nonlinear, Soft Matter Phys.* **87**, 052707. (doi:10.1103/PhysRevE.87.052707)
163. Rejniak K, Dillon R. 2007 A single cell-based model of the ductal tumour microarchitecture. *Comput. Math. Methods Med.* **8**, 51–69. (doi:10.1080/17486700701303143)
164. Powathil GG, Swat M, Chaplain MA. 2015 Systems oncology: towards patient-specific treatment regimes informed by multiscale mathematical modelling. *Semin. Cancer Biol.* **30**, 13–20. (doi:10.1016/j.semcancer.2014.02.003)
165. Powathil GG, Adamson DJ, Chaplain MA. 2013 Towards predicting the response of a solid tumour to chemotherapy and radiotherapy treatments: clinical insights from a computational model. *PLoS Comput. Biol.* **9**, e1003120. (doi:10.1371/journal.pcbi.1003120)
166. Kim Y, Kang H, Powathil G, Kim H, Trucu D, Lee W, Lawler S, Chaplain M. 2018 Role of extracellular matrix and microenvironment in regulation of tumor growth and LAR-mediated invasion in glioblastoma. *PLoS ONE* **13**, e0204865. (doi:10.1371/journal.pone.0204865)
167. Athale C, Mansury Y, Deisboeck TS. 2005 Simulating the impact of a molecular 'decision-process' on cellular phenotype and multicellular patterns in brain tumors. *J. Theor. Biol.* **233**, 469–481. (doi:10.1016/j.jtbi.2004.10.019)
168. Athale CA, Deisboeck TS. 2006 The effects of EGF-receptor density on multiscale tumor growth patterns. *J. Theor. Biol.* **238**, 771–779. (doi:10.1016/j.jtbi.2005.06.029)
169. Wang Z, Zhang L, Sagotsky J, Deisboeck TS. 2007 Simulating non-small cell lung cancer with a multiscale agent-based model. *Theor. Biol. Med. Modell.* **4**, 50. (doi:10.1186/1742-4682-4-50)
170. Kim Y, Stolarska MA, Othmer HG. 2011 The role of the microenvironment in tumor growth and invasion. *Prog. Biophys. Mol. Biol.* **106**, 353–379. (doi:10.1016/j.pbiomolbio.2011.06.006)
171. Kim Y, Roh S. 2013 A hybrid model for cell proliferation and migration in glioblastoma. *Discrete Contin. Dyn. Syst. Ser. B* **4**, 969–1015.
172. Kim Y, Powathil G, Kang H, Trucu D, Kim H, Lawler S, Chaplain M. 2015 Strategies of eradicating glioma cells: a multi-scale mathematical model with miR-451-AMPK-mTOR control. *PLoS ONE* **10**, e0114370. (doi:10.1371/journal.pone.0114370)
173. Caiazzo A, Ramis-Conde I. 2015 Multiscale modelling of palisade formation in glioblastoma multiforme. *J. Theor. Biol.* **383**, 145–156. (doi:10.1016/j.jtbi.2015.07.021)
174. Szabó A, Merks RMH. 2017 Blood vessel tortuosity selects against evolution of aggressive tumor cells in confined tissue environments: a modeling approach. *PLoS Comput. Biol.* **13**, e1005635. (doi:10.1371/journal.pcbi.1005635)
175. Engblom S, Wilson DB, Baker RE. 2018 Scalable population-level modelling of biological cells incorporating mechanics and kinetics in continuous time. *R. Soc. Open Sci.* **5**, 180379. (doi:10.1098/rsos.180379)
176. May C, Kolokotroni E, Stamatakis G, Büchler P. 2011 Coupling biomechanics to a cellular level model: an approach to patient-specific image driven multi-scale and multi-physics tumor simulation. *Prog. Biophys. Mol. Biol.* **107**, 193–9. (doi:10.1016/j.pbiomolbio.2011.06.007)
177. Zhang L, Strouthos CG, Wang Z, Deisboeck TS. 2009 Simulating brain tumor heterogeneity with a multiscale agent-based model: linking molecular signatures, phenotypes and expansion rate. *Math. Comput. Modell.* **49**, 307–319. (doi:10.1016/j.mcm.2008.05.011)
178. Chen WW, Niepel M, Sorger PK. 2010 Classic and contemporary approaches to modeling biochemical reactions. *Genes Dev.* **24**, 1861–75. (doi:10.1101/gad.1945410)
179. Kim Y, Stolarska M, Othmer H. 2007 A hybrid model for tumor spheroid growth in vitro i: theoretical development and early results. *Math. Models Methods Appl. Sci.* **17**, 1773–1798. (doi:10.1142/S0218202507002479)
180. Stolarska MA, Kim Y, Othmer HG. 2009 Multi-scale models of cell and tissue dynamics. *Phil. Trans. Ser. A, Math., Phys., Eng. Sci.* **367**, 3525–3553.
181. Erban R. 2016 Coupling all-atom molecular dynamics simulations of ions in water with Brownian dynamics. *Proc. R. Soc. London, Ser. A* **472**, 20150556.
182. Bearer EL, Lowengrub JS, Frieboes HB, Chuang YL, Jin F, Wise SM, Ferrari M, Agus DB, Cristini V. 2009 Multiparameter computational modeling of tumor invasion. *Cancer Res.* **69**, 4493–4501. (doi:10.1158/0008-5472.CAN-08-3834)
183. Frieboes HB, Jin F, Chuang YL, Wise SM, Lowengrub JS, Cristini V. 2010 Three-dimensional multispecies nonlinear tumor growth-II: tumor invasion and angiogenesis. *J. Theor. Biol.* **264**, 1254–1278. (doi:10.1016/j.jtbi.2010.02.036)
184. Rocha HL, Godet I, Kurtoglu F, Metzcar J, Konstantinopoulos K, Bhojyar S, Gilkes DM, Macklin P. 2021 A persistent invasive phenotype in post-hypoxic tumor cells is revealed by novel fate-mapping and computational modeling. *iScience* **24**, 102935. (doi:10.1016/j.isci.2021.102935)
185. Klank R, Rosenfeld S, Odde D. 2018 A Brownian dynamics tumor progression simulator with application to glioblastoma. *Convergent Sci. Phys. Oncol.* **4**, 015001. (doi:10.1088/2057-1739/aa9e6e)
186. Zhang L, Chen LL, Deisboeck TS. 2009 Multi-scale, multi-resolution brain cancer modeling. *Math. Comput. Simul.* **79**, 2021–2035. (doi:10.1016/j.matcom.2008.09.007)
187. Zhang L, Jiang B, Wu Y, Strouthos C, Sun PZ, Su J, Zhou X. 2011 Developing a multiscale, multi-resolution agent-based brain tumor model by graphics processing units. *Theor. Biol. Med. Modell.* **8**, 46. (doi:10.1186/1742-4682-8-46)
188. Rolls E, Erban R. 2017 Multi-resolution polymer Brownian dynamics with hydrodynamic interactions. *J. Chem. Phys.* **148**, 194111. (doi:10.1063/1.5018595)
189. Smith CA, Yates CA. 2018 Spatially extended hybrid methods: a review. *J. R. Soc. Interface* **15**, 20170931. (doi:10.1098/rsif.2017.0931)
190. Yates CA, George A, Jordana A, Smith CA, Duncan AB, Zygalakis KC. 2020 The blending region hybrid framework for the simulation of stochastic reaction–diffusion processes. *J. R. Soc. Interface* **17**, 20200563. (doi:10.1098/rsif.2020.0563)
191. Kavousanakis ME, Liu P, Boudouvis AG, Lowengrub J, Kevrekidis IG. 2012 Efficient coarse simulation of a growing avascular tumor. *Phys. Rev. E, Stat., Nonlinear, Soft Matter Phys.* **85**(3 Pt 1), 031912. (doi:10.1103/PhysRevE.85.031912)
192. Aviziotis I, Kavousanakis M, Bitsanis I, Boudouvis A. 2015 Coarse-grained analysis of stochastically simulated cell populations with a positive feedback genetic network architecture. *J. Math. Biol.* **70**, 1457–1484. (doi:10.1007/s00285-014-0799-2)
193. Van Liedekerke P, Neitsch J, Johann T, Alessandri K, Nassoy P, Drasdo D. 2019 Quantitative cell-based model predicts mechanical stress response of growing tumor spheroids over various growth conditions and cell lines. *PLoS Comput. Biol.* **15**, e1006273. (doi:10.1371/journal.pcbi.1006273)
194. Martínez AH, Madurga R, García-Romero N, Ayuso-Sacido Á. 2022 Unravelling glioblastoma heterogeneity by means of single-cell RNA sequencing. *Cancer Lett.* **527**, 66–79. (doi:10.1016/j.canlet.2021.12.008)
195. Stamatakis GS, Antipas VP, Uzunoglu NK. 2006 A spatiotemporal, patient individualized simulation model of solid tumor response to chemotherapy *in vivo*: the paradigm of glioblastoma multiforme treated by temozolomide. *IEEE Trans. Biomed. Eng.* **53**, 1467–1477. (doi:10.1109/TBME.2006.873761)
196. Stamatakis G, Antipas V, Uzunoglu N, Dale R. 2006 A four-dimensional computer simulation model of the *in vivo* response to radiotherapy of glioblastoma multiforme: studies on the effect of clonogenic cell density. *Br. J. Radiol.* **79**, 389–400. (doi:10.1259/bjr/30604050)
197. Lee JS *et al.* 2015 The complexities of agent-based modeling output analysis. *J. Artif. Soc. Soc. Simul.* **18**, jasss2897.
198. Jørgensen ACS, Ghosh A, Sturrock M, Shahrezaei V. 2022 Efficient Bayesian inference for stochastic agent-based models. *PLoS Comput. Biol.* **18**, e1009508. (doi:10.1371/journal.pcbi.1009508)
199. Oriapoulou ME, Tzamali E, Tzedakis G, Liapis E, Zacharakis G, Vakis A, Papamatheakis J, Sakkalis V. 2018 Integrating *in vitro* experiments with *in silico* approaches for glioblastoma invasion: the role of cell-to-cell adhesion heterogeneity. *Sci. Rep.* **8**, 16200. (doi:10.1038/s41598-018-34521-5)
200. Harpold HLP, Alvord EC, Swanson KR. 2007 The evolution of mathematical modeling of glioma proliferation and invasion. *J. Neuropathol. Exp. Neurol.* **66**, 1–9. (doi:10.1097/nen.0b013e31802d9000)
201. Wang C *et al.* 2009 Prognostic significance of growth kinetics in newly diagnosed glioblastomas revealed by combining serial imaging with a novel biomathematical model. *Cancer Res.* **69**, 9133–40. (doi:10.1158/0008-5472.CAN-08-3863)



202. Angeli S, Emblem KE, Due-Tonnessen P, Stylianopoulos T. 2018 Towards patient-specific modeling of brain tumor growth and formation of secondary nodes guided by DTI-MRI. *NeuroImage Clin.* **20**, 664–673. (doi:10.1016/j.nicl.2018.08.032)
203. Lipkova J *et al.* 2019 Personalized radiotherapy design for glioblastoma: integrating mathematical tumor models, multimodal scans, and Bayesian inference. *IEEE Trans. Med. Imaging* **38**, 1875–1884. (doi:10.1109/TMI.2019.2902044)
204. Ezhov I *et al.* 2021 Learn-Morph-Infer: a new way of solving the inverse problem for brain tumor modeling. (<http://arxiv.org/abs/2111.04090>).
205. Reiker T, Golumbeanu M, Shattock A, Burgert L, Smith TA, Filippi S, Cameron E, Penny MA. 2021 Emulator-based Bayesian optimization for efficient multi-objective calibration of an individual-based model of malaria. *Nat. Commun.* **12**, 7212. (doi:10.1038/s41467-021-27486-z)
206. Brennan C *et al.* 2013 The somatic genomic landscape of glioblastoma. *Cell* **155**, 462–477. (doi:10.1016/j.cell.2013.09.034)
207. McLendon R *et al.* 2008 Comprehensive genomic characterization defines human glioblastoma genes and core pathways. *Nature* **455**, 1061–1068. (doi:10.1038/nature07385)
208. Brooks LJ *et al.* 2021 The white matter is a pro-differentiative niche for glioblastoma. *Nat. Commun.* **12**, 1–14.
209. Neftel C *et al.* 2019 An integrative model of cellular states, plasticity, and genetics for glioblastoma. *Cell* **178**, 835–849. (doi:10.1016/j.cell.2019.06.024)
210. Bhaduri A *et al.* 2020 Outer radial glia-like cancer stem cells contribute to heterogeneity of glioblastoma. *Cell Stem Cell* **26**, 48–63. (doi:10.1016/j.stem.2019.11.015)
211. Couturier CP *et al.* 2020 Single-cell RNA-seq reveals that glioblastoma recapitulates a normal neurodevelopmental hierarchy. *Nat. Commun.* **11**, 1–19.
212. White K *et al.* 2020 New hints towards a precision medicine strategy for IDH wild-type Glioblastoma. *Ann. Oncol.: Offic. J. Europ. Soc. Med. Oncol.* **31**, 1679–1692. (doi:10.1016/j.annonc.2020.08.2336)
213. Xie Y *et al.* 2021 Key molecular alterations in endothelial cells in human glioblastoma uncovered through single-cell RNA sequencing. *JCI Insight* **6**, e150861. (doi:10.1172/jci.insight.150551)
214. Richards LM *et al.* 2021 Gradient of developmental and injury response transcriptional states defines functional vulnerabilities underpinning glioblastoma heterogeneity. *Nat. Cancer* **2**, 157–173. (doi:10.1038/s43018-020-00154-9)
215. Kaminska B, Ochocka N, Segit P. 2021 Single-cell omics in dissecting immune microenvironment of malignant gliomas—challenges and perspectives. *Cells* **10**, 2264. (doi:10.3390/cells10092264)
216. Karaayvaz M *et al.* 2018 Unravelling subclonal heterogeneity and aggressive disease states in TNBC through single-cell RNA-seq. *Nat. Commun.* **9**, 3588. (doi:10.1038/s41467-018-06052-0)
217. Ravi VM *et al.* 2022 Spatially resolved multi-omics deciphers bidirectional tumor-host interdependence in glioblastoma. *Cancer Cell* **40**, 639–655. (doi:10.1016/j.ccell.2022.05.009)
218. Wende T, Hoffmann KT, Meixensberger J. 2020 Tractography in neurosurgery: a systematic review of current applications. *J. Neurol. Surg. Part A, Central Europ. neurosurg.* **81**, 442–455. (doi:10.1055/s-0039-1691823)
219. Jiang H, Yu K, Li M, Cui Y, Ren X, Yang C, Zhao X, Lin S. 2020 Classification of progression patterns in glioblastoma: analysis of predictive factors and clinical implications. *Front. Oncol.* **10**, 590648. (doi:10.3389/fonc.2020.590648)
220. Nie S *et al.* 2021 Determining optimal clinical target volume margins in high-grade glioma based on microscopic tumor extension and magnetic resonance imaging. *Radiat. Oncol. (London, England)* **16**, 97. (doi:10.1186/s13014-021-01819-0)
221. Vivas-Buitrago T *et al.* 2022 Influence of supramarginal resection on survival outcomes after gross-total resection of IDH-wild-type glioblastoma. *J. Neurosurg.* **136**, 1–8. (doi:10.3171/2020.10.JNS203366)
222. Louis DN *et al.* 2021 The 2021 WHO classification of tumors of the central nervous system: a summary. *Neuro Oncol.* **23**, 1231–1251. (doi:10.1093/neuonc/noab106)
223. Lueckmann JM, Boelts J, Greenberg DS, Gonçalves PJ, Macke JH. 2021 Benchmarking simulation-based inference. (<http://arxiv.org/abs/2101.04653>).
224. Enderling H, Wolkenhauer O. 2020 Are all models wrong? *Comput. Syst. Oncol.* **1**. (doi:10.1002/cso2.1008)
225. Jiménez-Sánchez J *et al.* 2021 A mesoscopic simulator to uncover heterogeneity and evolutionary dynamics in tumors. *PLoS Comput. Biol.* **17**, e1008266. (doi:10.1371/journal.pcbi.1008266)
226. Coggan H, Page KM. 2022 The role of evolutionary game theory in spatial and non-spatial models of the survival of cooperation in cancer: a review. *J. R. Soc. Interface* **19**, 20220346. (doi:10.1098/rsif.2022.0346)